THE UNIVERSITY OF ALBERTA

DEFORMATION CHARACTERISTICS OF PRETENSIONED CONCRETE BEAMS IN FLEXURE

by

GEORGE RAFFA

A THESIS

SUBMITTED TO THE FACULTY OF GRADUATE STUDIES

IN PARTIAL FULFILMENT OF THE REQUIREMENTS FOR THE DEGREE

OF MASTER OF SCIENCE

DEPARTMENT OF CIVIL ENGINEERING

EDMONTON, ALBERTA

OCTOBER, 1964

UNIVERSITY OF ALBERTA

FACULTY OF GRADUATE STUDIES

The undersigned certify that they have read, and recommend to the Faculty of Graduate Studies for acceptance, a thesis entitled "DEFORMATION CHARACTERISTICS OF PRETENSIONED CONCRETE BEAMS IN FLEXURE" submitted by GEORGE RAFFA in partial fulfilment of the requirements for the degree of MASTER OF SCIENCE.

ABSTRACT

The object of this thesis was to study the deformation characteristics of bonded, prestressed concrete beams loaded in flexure. Of particular interest was the moment-curvature relationship.

All beams had a 6 x 12-in. cross-section and an effective depth of 10 in. Six of the beams were loaded at two points symmetrical about midspan and had a span length of 11 ft. The remaining four beams were loaded at midspan only. Two of these beams had an 11-ft. span and the other two a span of 56-in.

For the two-point loaded beams the percentage of reinforcement was varied from 0.19 to 0.58 and two levels of concrete strength were used. All the one-point loaded beams had reinforcement ratios of 0.38; the concrete strength was varied as for the two-point loaded beams.

The load-deformation relationships exhibited three distinct stages of behavior. The amount of reinforcement had a considerable effect on the extent of these stages.

Further investigation is required to study the behavior of similar beams having a concrete strength on the order of 3000 psi.

ACKNOWLEDGEMENTS

This project was made possible through facilities and equipment provided by the University in the new Structural Laboratory. Financial assistance given by the National Research Council of Canada is gratefully acknowledged.

This thesis was supervised by Dr. J. Warwaruk, Associate Professor in the Department of Civil Engineering. His guidance and assistance throughout the program are sincerely appreciated.

The author wishes to thank the technicians who helped in making up the equipment and in the fabrication and testing of the specimens.

The author wishes to thank his wife for typing the manuscript.

TABLE OF CONTENTS

TABLE OF CONTENTS (continued)

TABLE OF CONTENTS (continued)

LIST OF TABLES

LIST OF FIGURES

LIST OF FIGURES (continued)

LIST OF FIGURES (continued)

CHAPTER 1

INTRODUCTION

1.1. Introductory Remarks

With the advent of ultimate strength procedures in prestressed concrete design and analysis, research has been directed toward the determination of experimental factors necessary for predicting the strength of prestressed concrete beams. A general flexural strength analysis for unbonded, partially bonded, and fully bonded prestressed concrete beams was advanced in 1962, (1)*. However, of equal importance is the deformation aspect. In this field of beam behavior little work has been done, particularly in the region of curvature.

Curvature as used here is the rate of change of slope of the beam per unit length of the beam. When curvature is combined with the corresponding moment, the resulting moment-curvature relationship can be used to predict the behavior of a beam.

1.2. Object

This thesis represents a pilot investigation which will be used for comparison purposes and as a basis for future research.

---

*The numbers in parenthesis refer to the entries in the List of References.

The major variables investigated were:

(1) amount of tension reinforcement,

(2) concrete strength,

(3) type of loading: one-point or two-point,

(4) and shear-to-moment ratio for the one-point loaded beams.

Though not intended, there was some variation in the amount of effective prestress for the two-point loaded beams. The effect of these variables on the distribution of strain in the extreme concrete fiber, on the distribution of strain over the depth of the beam, and on the load-deflection curves was studied. In addition, moment-curvature relationships were computed from both the measured strains and deflections. Theoretical moment-curvature relationships were determined and compared with those computed from the deflections.

1.3. Scope

A total of 10 rectangular beams of 6 x 12-in. cross-section were tested. Each beam was reinforced in tension with either 2, 4, or 6 strands of 5/16 in. nominal diameter, 7-wire strand with a yield strength of 245 ksi (0.2 per cent offset) and an ultimate strength of 270 ksi. The effective depth to the reinforcement was maintained constant at 10 in.

Beams* No. 1 to 6 represented a series involving three reinforcement percentages, 0.19, 0.38, and 0.58 per cent, and two concrete strengths,

---

*The beams were numbered from one to ten in order of casting with the higher concrete strength beams being cast first.

approximately 6500 and 5000 psi. These were loaded at two points, 3-ft. from each support, resulting in a central 5-ft. span having a constant moment; i.e. zero shear. The end 3-ft. spans were reinforced with stirrups to prevent failure in shear.

Beams No. 7 to 10 were loaded with a concentrated load at midspan. Each beam had a reinforcement ratio of 0.38 per cent (4 strands) and was reinforced with stirrups throughout its entire length. Beams No. 7 and 8 had an 11-ft. span between supports with 7500 and 5400 psi concrete, respectively, while beams No. 9 and 10 had a 56-in. span with 6200 and 4300 psi concrete, respectively.

About 20 per cent of the total time spent on this thesis was devoted to the construction of a prestressing bed made up of two heavily reinforced concrete end blocks anchored down to the loading bed by pre-stressed bolts. Details are given in Appendix B.

CHAPTER 11

LITERATURE REVIEW

2.1. Introductory Remarks

The major field of interest in this thesis is that of deformation characteristics of bonded, prestressed concrete beams and in particular the moment-curvature relationships. In this latter area little direct work has been done except in connection with moment redistribution characteristics of continuous beams. A very extensive program was completed at the University of Illinois (1), (3) from 1951 to 1959 which included aspects of both strength and deformation characteristics of beams loaded in flexure.

Strength has been the major concern of investigators working with prestressed concrete and it has not been until recently with the introduction of Limit Design procedures into European codes that research has felt the need to investigate the factors influencing the rotation capacities of prestressed concrete sections. Rotation capacity is also a very important aspect in the design of structures to withstand earthquakes and blasts.

2.2. Research in Moment Redistribution

In 1957, Giorgio Macchi (2) described the tests which had been carried out in Turin on three prestressed beams continuous over three spans and on a simply supported control beam. The beams were tested to failure by applying two equal point loads very near to the midspan. The object of

the tests was to study certain aspects of moment redistribution. Using the equations of equilibrium supplemented with certain assumptions, he determined a theoretical moment-curvature diagram which he suggested could be idealized with three sloping straight lines. His conclusions included the opinion that the only condition for the establishment of practical design methods is the experimental checking of some assumptions concerning the calculation of rotations and the improvement of the method of plotting the moment-curvature diagram.

2.3. Research in Strength Analysis

2.3.1. D. F. Billet and J. H. Appleton (3) in 1954 reported on a project carried out at the University of Illinois. It consisted of tests on 26 rectangular bonded, post-tensioned concrete beams loaded at the third points of a 9-ft. simple span. The effect of percentage of steel, amount of prestress, and concrete strength on deflections, cracking loads, and ultimate loads were studied.

A flexural strength analysis was developed and the effect of varying the parameters used in the analysis was examined in terms of ultimate strength.

The results of the beam tests reported here were included in those studied in (1).

2.3.2. An investigation (4) on prestressed concrete beams was conducted by the Portland Cement Association in 1953-54. Based on experimental and analytical studies, the relative performances of pre-tensioned, post-tensioned grouted, post-tensioned unbonded, post-tensioned unbonded with deformed bars added, and conventional bar reinforcement

were compared in terms of moment-deflection relationships, deflection recovery, and ultimate strength of beams failing in flexure for three reinforcement percentages. The 19 beams had 9-ft. spans and were tested for third-point loading.

The strengths of the pre-tensioned and corresponding post-tensioned bonded beams were nearly equal, and 20 to 40 per cent higher than the strength of corresponding unbonded post-tensioned beams. Unbonded beams tested in which one strand was replaced by embedded deformed bars gave ultimate strengths close to those of corresponding bonded prestressed beams. The prestress transfer length developed when 3/8-in. rusted strand was released into 4000 psi concrete was not greater than 12 in.

2.3.3. A most extensive investigation of the strength and behavior of prestressed concrete beams was undertaken at the University of Illinois during the period 1951 to 1959. A total of 82 rectangular beams were reported on, involving bonded, unbonded, and partially bonded reinforcement. The major variables were: (1) amount of reinforcement, (2) concrete strength, (3) effective prestress, and (4) type of loading: loaded at midspan only or at two points symmetrical about midspan.

A general flexural strength analysis and procedures for the determination of flexural deformations at various stages of loading of prestressed concrete beams were presented. Simple approximate methods for the determination of flexural strength were also presented. In addition, a method for the determination of moment-curvature relationships for prestressed concrete beams throughout all stages of behavior was given.

2.4. Aspects of Moment Curvature

2.4.1. In 1963, N. H. Burns described a study of prestressed beams having different amounts of prestressing in terms of analytically derived moment-curvature relationships. The method of analysis was taken from reference (1) with the exception that a modified form of the Hognestad stress block was used and a constant limiting strain was chosen. It was suggested that the moment-curvature and hence the load-deflection relationships could be controlled by partial prestressing to satisfy the two stages of behavior, service load conditions and ultimate, somewhat independently of each other.

CHAPTER 111

THEORY

3.1. Beam Curvature

3.1.1. Curvature in terms of the deflected shape. Consider an element, dx, of the beam shown in FIGURE 3.1 (a). This element is shown in FIGURE 3.1 (b) after an arbitrary load has been applied to the beam.

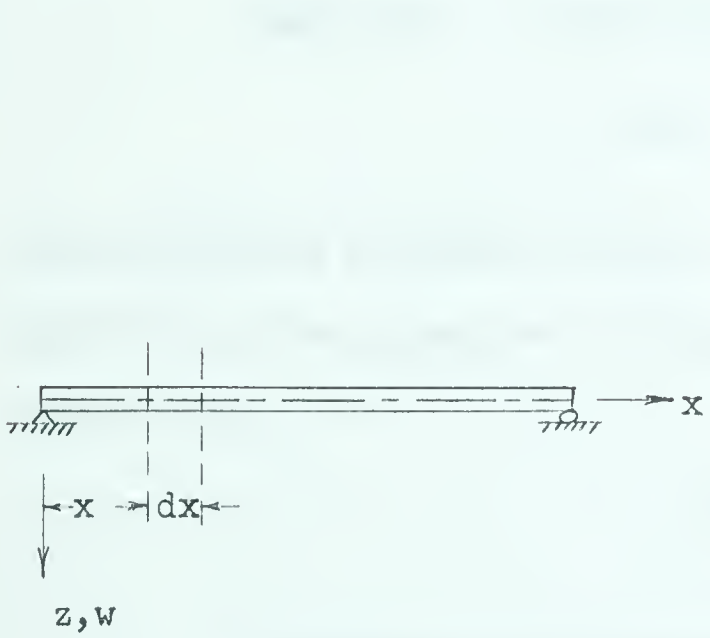

(a) Beam before load applied.

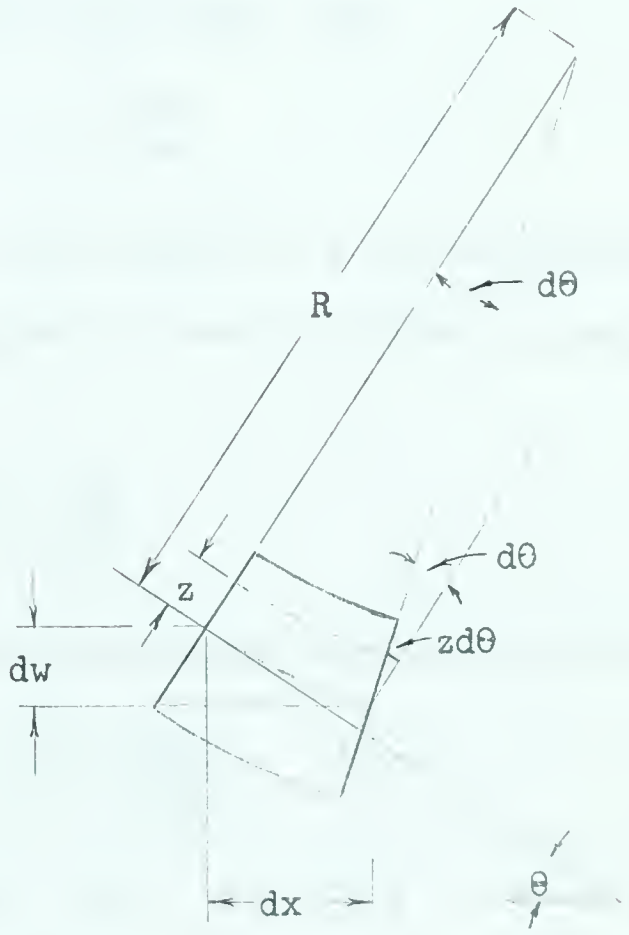

(b) Element, dx, after loading.

FIGURE 3.1. GEOMETRY OF A BEAM BEFORE AND AFTER LOADING

If the deflection, w, is small compared to the length of the beam, then

$$R\,d\theta = dx \text{ or } \frac{d\theta}{dx} = \frac{1}{R} \tag{3.1}$$

where 1/R is designated as the "curvature".

Let ϵ_x be the strain at a distance, z, from the neutral axis. If tension is taken as positive, then

$$z d\theta = -\epsilon_x dx \text{ or } \frac{d\theta}{dx} = \frac{-\epsilon_x}{z} \tag{3.2}$$

Substituting EQUATION (3.2) into EQUATION (3.1), the curvature is obtained in terms of strain

$$\frac{1}{R} = \frac{-\epsilon_x}{z} \tag{3.3}$$

Once again, if deflections are small, then

$$\tan\theta = \theta = \frac{dw}{dx} \tag{3.4}$$

Differentiating EQUATION 3.4 once with respect to x and substituting into EQUATION 3.1 the curvature is obtained in terms of deflection as given in EQUATION 3.5.

$$\frac{1}{R} = \frac{d^2w}{dx^2} \tag{3.5}$$

In summary, the following expressions have been derived:

$$\frac{1}{R} = \frac{d\theta}{dx} = \frac{-\epsilon_x}{z} = \frac{d^2w}{dx^2} \tag{3.6}$$

3.1.2. C u r v a t u r e i n t e r m s o f m o m e n t.

From the theory of elasticity and Hooke's Law

$$\sigma_x = E\epsilon_x \tag{3.7}$$

where σ_x is the stress at a distance, z, from the neutral axis and E is

the modulus of elasticity. The moment at the section considered is given by the integral

$$M = \int_{-\frac{b}{2}}^{+\frac{b}{2}} \sigma_x \, b \, z \, dz \qquad (3.8)$$

where b is the width of the beam. By combining EQUATION 3.6, EQUATION 3.7, and EQUATION 3.8, the following relationship is obtained:

$$M = -EI \frac{d^2w}{dx^2} \qquad (3.9)$$

where I is the moment of inertia of the cross-section about its centroidal axis.

In summary, the following expressions have been determined:

$$\frac{1}{R} = \frac{-M}{EI} = \frac{d^2w}{dx^2} \qquad (3.10)$$

3.2. Effect of Cracking on Strain and Curvature

The limitations of the elastic theory require that all sections remain homogeneous throughout the period of loading. However, in pre-stressed concrete such is not the case because of cracking which occurs in later stages of loading. This results in some sections consisting of a zone of concrete in compression and the tension reinforcement while other sections remain essentially homogeneous. A somewhat idealized cracking pattern is shown in FIGURE 3.2 (a) for a prestressed beam with a central constant moment region.

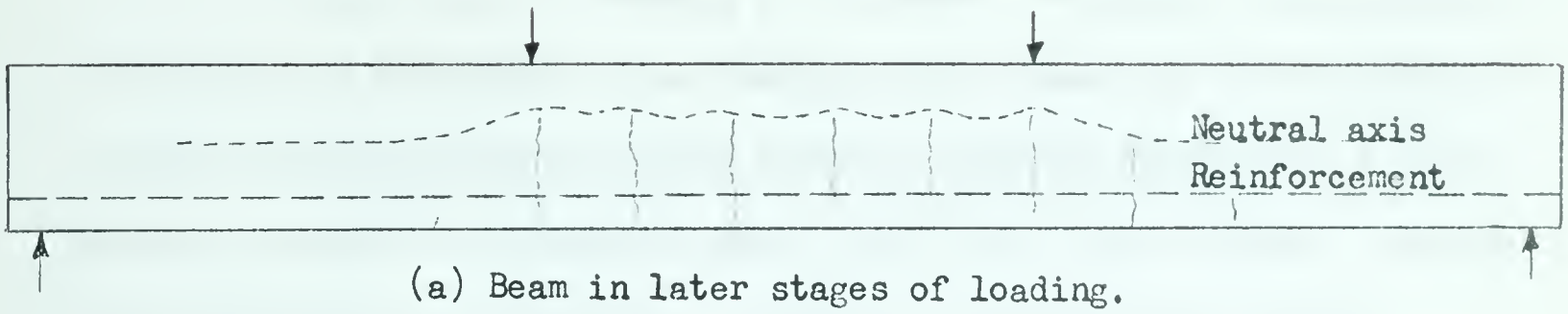

(a) Beam in later stages of loading.

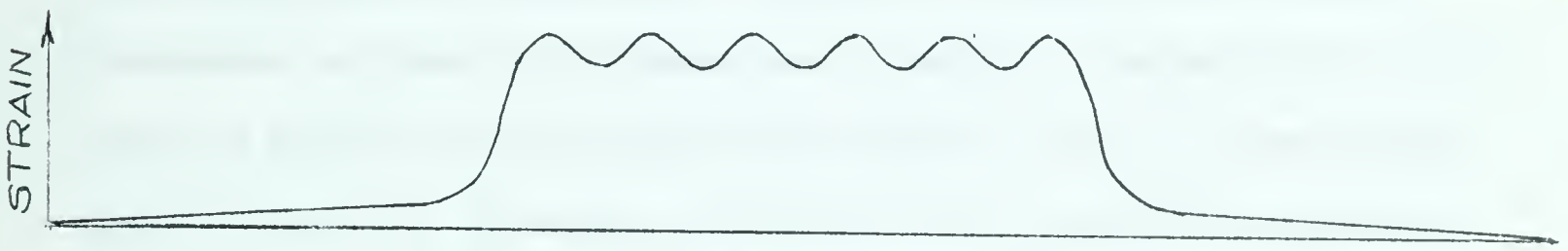

(b) Distribution of strain in the extreme concrete fiber along the span.

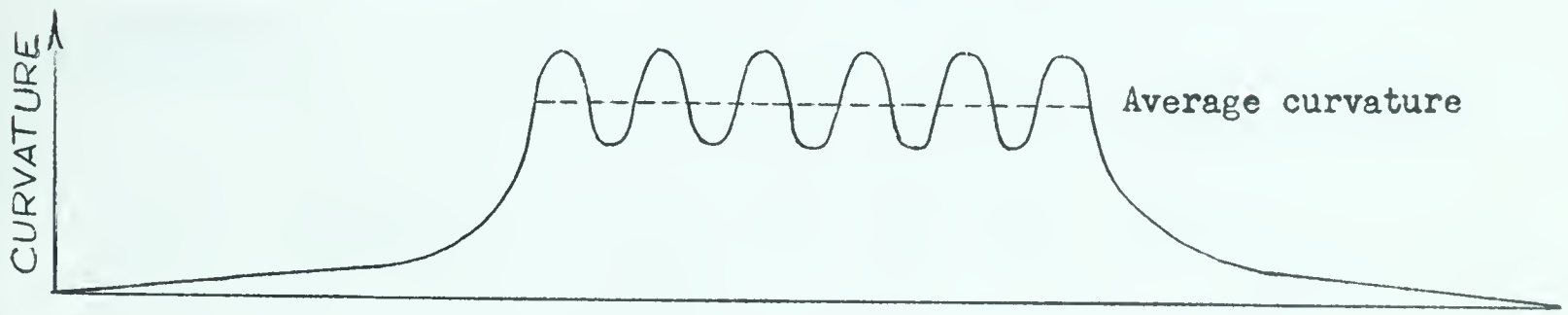

(c) Distribution of curvature along the span.

FIGURE 3.2. DISTRIBUTION OF STRAIN AND CURVATURE ALONG A SPAN.

Because concrete does have strength in tension, the neutral axis is lower between cracks than at the head of the cracks. With the larger compression zone between cracks, the concrete strains are smaller in these regions as shown in FIGURE 3.2 (b). Since curvature is defined as the ratio of the strain in the extreme fiber to the depth to the neutral axis (EQUATION 3.3), a low neutral axis and a small strain combine to give a small curvature in the regions between cracks, while at the cracked sections the resulting curvature is much larger as shown in FIGURE 3.2 (c).

The effect of cracking is to cause a variance in the magnitude of strains and curvatures along the span which means that the assumption of plane sections remaining plane cannot be applied directly to a given section, though the assumption should hold true if the "average" strains and curvatures are considered. A method of working with "average" curvatures is given in (1) where use is made of a compatibility factor which is defined as the ratio of the change in strain in the extreme concrete fibre to the change in strain in the tension reinforcement. This theory concerning the effects of cracks is further discussed in CHAPTER V.

CHAPTER IV

MATERIALS, FABRICATION, AND TESTING PROCEDURE

4.1. Materials

4.1.1. C e m e n t. Type III cement was used in all mixes. It was purchased from a local manufacturer and delivered to the Structural Laboratory just prior to the commencement of the project.

4.1.2. A g g r e g a t e. The sand had a fineness modulus of 2.54 which was determined by means of a sieve analysis. The grading fell between limits set by ASTM (6). At the start of the project the moisture content of the sand was 3.2 per cent. The coarse aggregate was crushed gravel with a maximum size of 3/4 in.

4.1.3. C o n c r e t e M i x e s. Mixes were designed on the basis of tables and charts given in "Design and Control of Concrete Mixtures" (7) with modifications made with the aid of trial mixes. Based on visual observation of the concrete in the mixes, minor adjustments in water content were made from beam to beam. In addition, the cement content of the lower strength concrete beams was progressively reduced in small amounts in an attempt to reduce the strength of the concrete. Properties of the concrete mixes are listed in Table 4.1.

4.1.4. R e i n f o r c e m e n t. High-strength 7-wire strand of 5/16 in. nominal diameter was used as tension reinforcement in all beams. It was purchased from British Ropes of Vancouver. A stress-strain

TABLE 4.1. PROPERTIES OF CONCRETE MIXES

Beam No.	Cement: Sand: Gravel by Weight	Water: Cement by Weight	Slump	Compressive Strength f'_c		Tensile Strength		Modulus of Rupture fr		Age at Test days	Compressive Strength 3-d	Compressive Strength 7-d
			in.	p.s.i.		p.s.i.		p.s.i.			p.s.i.	p.s.i.
				1	2	1	2	1	2			
1	1:1.6:1.9	0.49	5½	6840	6290	391	463	576	675	27	(4-d) 5340	6270
2	1:1.6:1.9	0.47	3½	6380	6560	480	471	675	643	29	5140	----
3	1:1.6:1.9	0.48	2½	7800	7900	495	517	832	697	25	5940	6640
4	1:3.1:3.3	0.70	4	4730	4880	372	342	586	596	24	2980	3930
5	1:3.1:3.3	0.68	6	5210	5210	372	400	694	610	23	(4-d) 3680	4730
6	1:3.2:3.3	0.68	2	5390	5400	360	427	581	631	21	3910	----
7	1:1.6:1.9	0.47	4½	7850	7400	495	383	719	774	20	----	6820
8	1:3.2:3.4	0.71	1	5370	5390	463	453	741	784	17	4110	4800
9	1:1.6:2.0	0.48	5	5520	6420	445	504	614	524	21	4800	5990
10	1:3.2:3.4	0.70	4	4210	4350	352	374	545	555	22	2680	3790

curve for this reinforcement is shown in FIGURE 4.1.

Stirrups consisting of No. 2 plain or No. 3 deformed bent bars were used to prevent a premature shear failure.

4.2. Fabrication of Test Specimens

4.2.1. F o r m i n g P r o c e d u r e. The bottom and two sides of the beam form were steel channel sections. The bottom flanges of the sides were bolted with 3/8-in. bolts at 2-ft. intervals to the web of the bottom channel, allowing relative ease in stripping and in assembly. A steel channel section was also used for the end plates which were drilled at the appropriate heights to allow the cables to pass through. They were held in place by means of clamps.

For beams No. 1 to 6 the form was set up and the stirrup cages placed in the form prior to prestressing. For beams No. 7 to 10 the strands were prestressed, the stirrups wired to the strands, and finally the sides of the form were set in position.

4.2.2. P r e s t r e s s i n g S t r a n d. The cables were prestressed individually with the use of a 30-ton Simplex center-hole hydraulic ram operated by a 10,000 psi Blackhawk hand pump which are shown in FIGURE 4.2. The force in the strands was measured with specially constructed aluminum dynamometers which are detailed in Appendix B. Loss of prestress from the time of prestressing to the time of casting was measured by the dynamometers.

The end anchorages for the strand were steel-constructed gripping devices. They consisted of an outer cylindrical casing with a tapered central hole which housed a three-piece circular wedge and a coil spring.

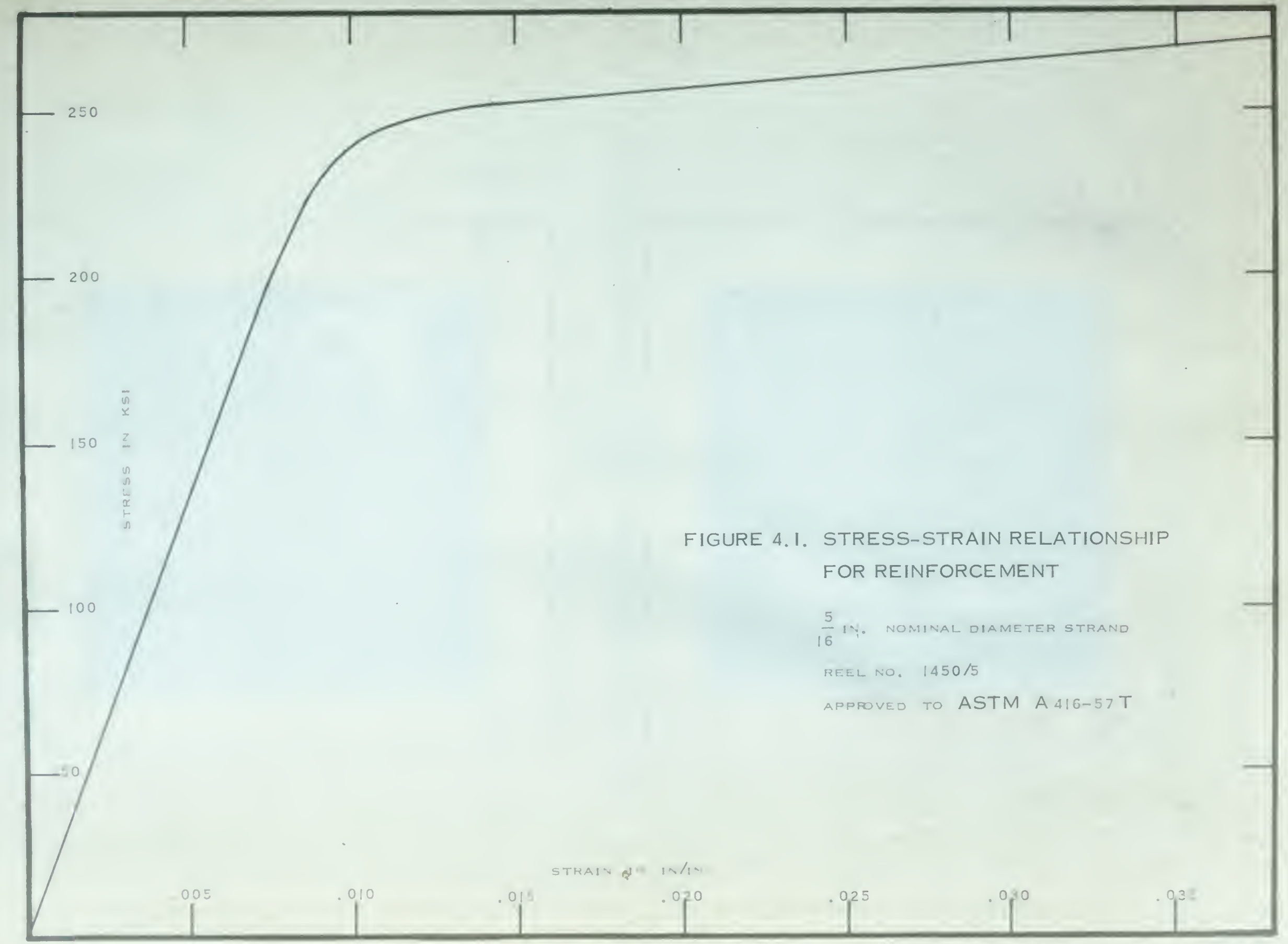

FIGURE 4.1. STRESS-STRAIN RELATIONSHIP FOR REINFORCEMENT

$\frac{5}{16}$ IN. NOMINAL DIAMETER STRAND

REEL NO. 1450/5

APPROVED TO ASTM A 416-57 T

FIGURE 4.2. JACKING ARRANGEMENT FOR PRESTRESSING STRAND [SOUTH END]

FIGURE 4.3. NORTH END OF PRESTRESSING BED SHOWING THE GRIPS AND DYNAMOMETERS

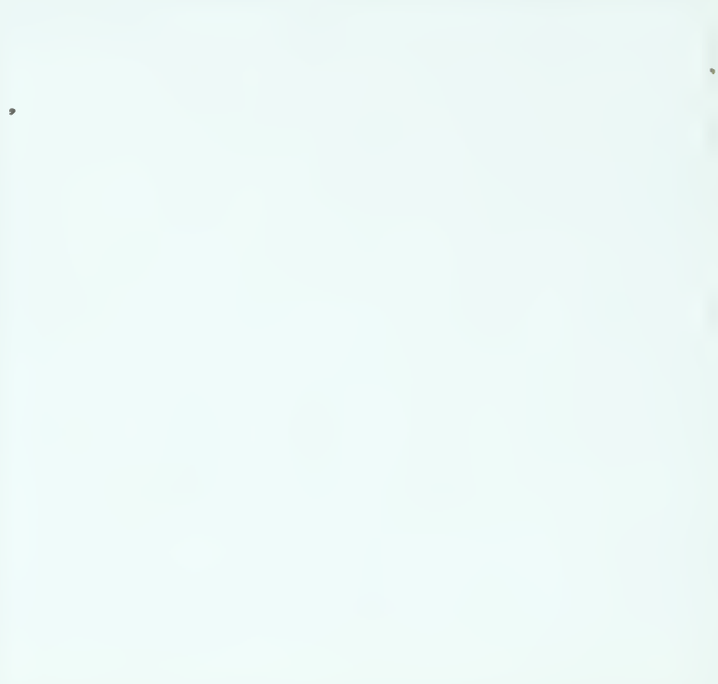

The inside of the wedge had grooves which gripped the strand as a result of the wedging action between the wedge and the casing when the prestressing force was applied. The spring acted between the end of the wedge and the inside of one end of the casing. This end of the casing was a removable threaded cap with a central 3/8 in. diameter hole. The purpose of the spring was to hold the wedge tight against the casing when bringing the grip into bearing against the end block. This feature was especially useful on the jacking end during the prestressing operation. Outside dimensions of the grips were: 1 1/4 in. in diameter by 3 1/2 in. long. A photograph of the north end of the prestressing bed showing the grips and dynamometers is presented in FIGURE 4.3.

4.2.3. B a t c h i n g P l a n t. Batching of the concrete mixes was carried out in the recently built structural laboratory using the new batching plant facilities which include bins for storing aggregates, a water storage tank, scales, and a 9-cu. ft. capacity non-tilting mixer. These facilities were put into operation for the first time with the batching of the concrete for the end blocks at the beginning of the project. Photographs of the batching plant are shown in FIGURES 4.4 and 4.5.

The five storage bins are elevated off the main floor so that a hopper can pass freely beneath. The hopper is suspended from a frame which in turn is attached by rollers to a track just below the bottom of the bins. By means of a system of knife edges, levers and linkages, a certain ratio of the weight of the hopper and its content is transferred to a scale which is fixed to the frame. The scale is calibrated to measure up to 1600 lb. of material in the hopper. The weight of water in the water tank is measured by a similar system, except that the scale is calibrated

FIGURE 4.4. BATCHING PLANT

FIGURE 4.5. BATCHING PLANT

to measure the weight of 240 lb. of water in the tank. An important feature of this system is that the scale reads zero when the tank is full and shows an increasing reading as water flows out of the tank. Thus, the amount of water entering the mixer can be determined directly from the scale. A system of pipes and valves makes it possible to run water into the tank from an outside source, or drain water from the tank into the mixer or into the sump. The water enters the mixer through a segment of perforated pipe to ensure a more uniform distribution of water in the mixer.

Aggregate which has been weighed in the hopper is dumped into a mixer bucket which runs on rollers up an inclined track and then dumps the aggregate into the mixer. Details for the handling of cement have not been finalized; consequently, the cement is placed by hand into the mixer bucket together with the aggregate. Where required, portions of a bag are weighed on a portable scale.

4.2.4. C a s t i n g o f t h e S p e c i m e n s. The procedure used in batching of the concrete is as follows. First, the dry materials were weighed and mixed for 1 to 2 minutes. Then, approximately 80 per cent of the total amount of water was added and the materials were mixed for an additional 2 minutes. The remaining amount of water, which depended upon design requirements and visual observation of the concrete in the mixer, was added and the mixing was continued for a final 1 to 2 minutes. A butter mix of approximately 2 cu. ft. and having the same proportions as the design mix was used to condition the mixer before batching of the beam mix. Slump determination was made immediately after batching of the beam mix.

One batch of 8 cu. ft. was sufficient to cast one beam,

six - 6 x 12 in. control cylinders, and two - 3 1/2 x 4 1/2 in. control beams. All concrete was compacted with an 11,500 rpm immersion type vibrator.

4.2.5. C u r i n g o f t h e S p e c i m e n s. At about the time of final set, the concrete was covered with a polythene sheet. The following day the forms were stripped and the beam and control specimens covered with wet burlap and a sheet of polythene. After moist curing for an additional two days, the covering was removed and they were stored in air until the time of test.

4.2.6. R e l e a s e o f P r e s t r e s s. The prestress was released from 3 to 4 days after casting. This was done by cutting the cables at one end with an acetylene torch. It was desirable that the prestress be released slowly, but the cables snapped quite rapidly under the high tension when the heat was applied. However, before release, two external cables were positioned at 2 in. from the top of the beam and pretensioned so that the tension was reduced in the top extreme fibre. In some cases, the top cables were unintentionally overstressed and the entire cross-section was put into compression when the bottom strands were released. No top cables were used for beam No. 1 because computations indicated that the tension was not large enough to produce cracking. Some cracking across the top of the beams in the end regions became visible after curing in air; these were assumed to be shrinkage cracks, particularly since they were found to occur in the region immediately above the stirrups.

4.2.7. C o n t r o l S p e c i m e n s. One control cylinder was tested in compression at each of 3 and 7 days after casting. On the day of the beam test, the two control beams and the four control cylinders

were tested: two in compression and two in splitting. The control cylinders were capped before performing the compression tests. The flexure specimens were tested with the 4 1/2 in. side horizontal. They were loaded at the third points of a twelve inch span; the overall length of the beams was 14 in.

4.2.8. Description of Test Specimens. A total of 10 rectangular prestressed beams were cast. All beams had a 6 x 12 in. cross-section and a constant effective depth of 10 in. The overall beam lengths were: Beams No. 1 to 8, 12' - 6" and beams No. 9 and 10, 71 in. Further details of the test specimens are given in Table 4.2.

TABLE 4.2. DETAILS OF TEST SPECIMENS

Beam No.	f'_c (psi)	Relative Concrete Strength	Amount of Reinforcement ($in.^2$)	$p=\frac{A_s}{bd}$	$\frac{p}{f'_c}$ (10^{-7} /psi)	Effective Prestress (ksi)
1	6560	High	.1154	.00193	2.94	142
2	6420	"	.2308	.00384	5.98	133
3	7850	"	.3462	.00578	7.36	120
4	4800	Low	.1154	.00193	4.02	139
5	5210	"	.2308	.00384	7.37	129
6	5390	"	.3462	.00578	10.7	123
7	7550	High	.2308	.00384	5.09	133
8	5380	Low	.2308	.00384	7.14	133
9	6200	High	.2308	.00384	6.20	134
10	4280	Low	.2308	.00384	8.98	133

Beams No. 1 to 6 were designed as one series. These beams were

loaded at two points which were 5 ft. apart and symmetrical about midspan. The total span length was 11 ft. For this series, an attempt was made to obtain two different levels of concrete strength. It was then proposed to study the effects on the behavior of the beams of concrete strength and amount of reinforcement for three percentages of reinforcement. The magnitude of the effective prestress was not intended to be a variable; however, some variation was obtained because of the higher losses which occurred in the more heavily reinforced beams.

Beams No. 7 to 10 were designed as another series which were loaded only at midspan. Beams No. 7 and 8 had an 11-ft. span; beams No. 9 and 10 a span of 56 in. All beams in this series had the same amount of tension reinforcement and the same effective prestress. Here, as in the first series, the effect of concrete strength was studied. In addition, the ratio of shear to moment was varied by making the lengths of beams No. 9 and 10 approximately one-half the length of beams No. 7 and 8. Another variable whose effects were indeterminable was the amount of shear reinforcement which varied between the long and short beams.

For beams No. 1 to 6, stirrup cages made up of the appropriate number of stirrups and four No. 3 straight bars were placed in the two outer regions as indicated in FIGURE 4.6.

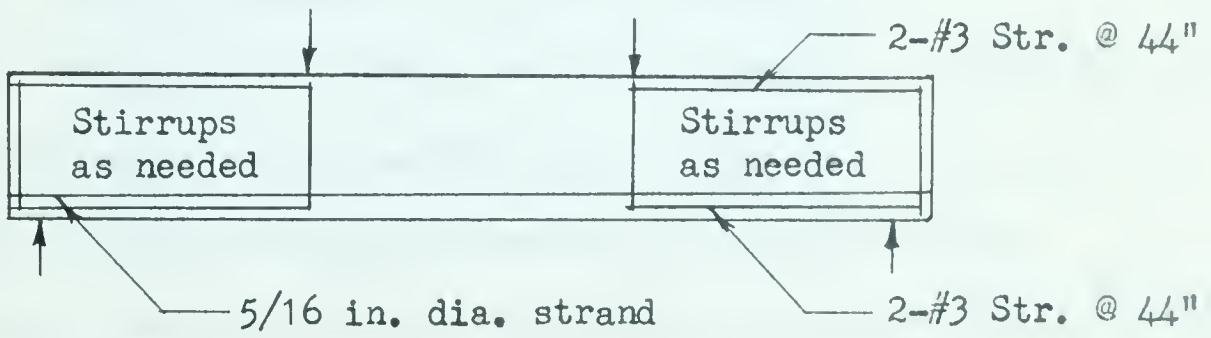

FIGURE 4.6. SHEAR REINFORCEMENT FOR BEAMS NO. 1 TO 6.

For beams No. 7 to 10, stirrups, wired at the bottom to the reinforcement, were placed over the entire length. Although two No. 3 straight bars were used at the top to help hold the stirrups in place during the placing of the concrete, they were removed when the forms were filled. The stirrup details for all beams are given in Table 4.3.

TABLE 4.3. DETAILS OF SHEAR REINFORCEMENT

Beam No.	Bar Size	Stirrup Spacing (in.)
1	#3	6 ½
2	#2	4 ½
3	#3	5
4	#2	5
5	#2	3 ½
6	#3	5
7	#2	6
8	#2	6
9	#2	3
10	#2	3

4.3. Testing Procedure

4.3.1. L o a d i n g A p p a r a t u s. The beams were simply supported. The end supports are shown in FIGURE 5.9.

Overall views of the loading setup are presented in FIGURES 4.7 and 4.8. For beams loaded at two points (Nos. 1 to 6), the load was applied by means of a distributing beam resting on a ball bearing between two-6 x 6-in. bearing plates on the north end and on a roller between another two-6 x 6-in. bearing plates at the south end. For the beams loaded

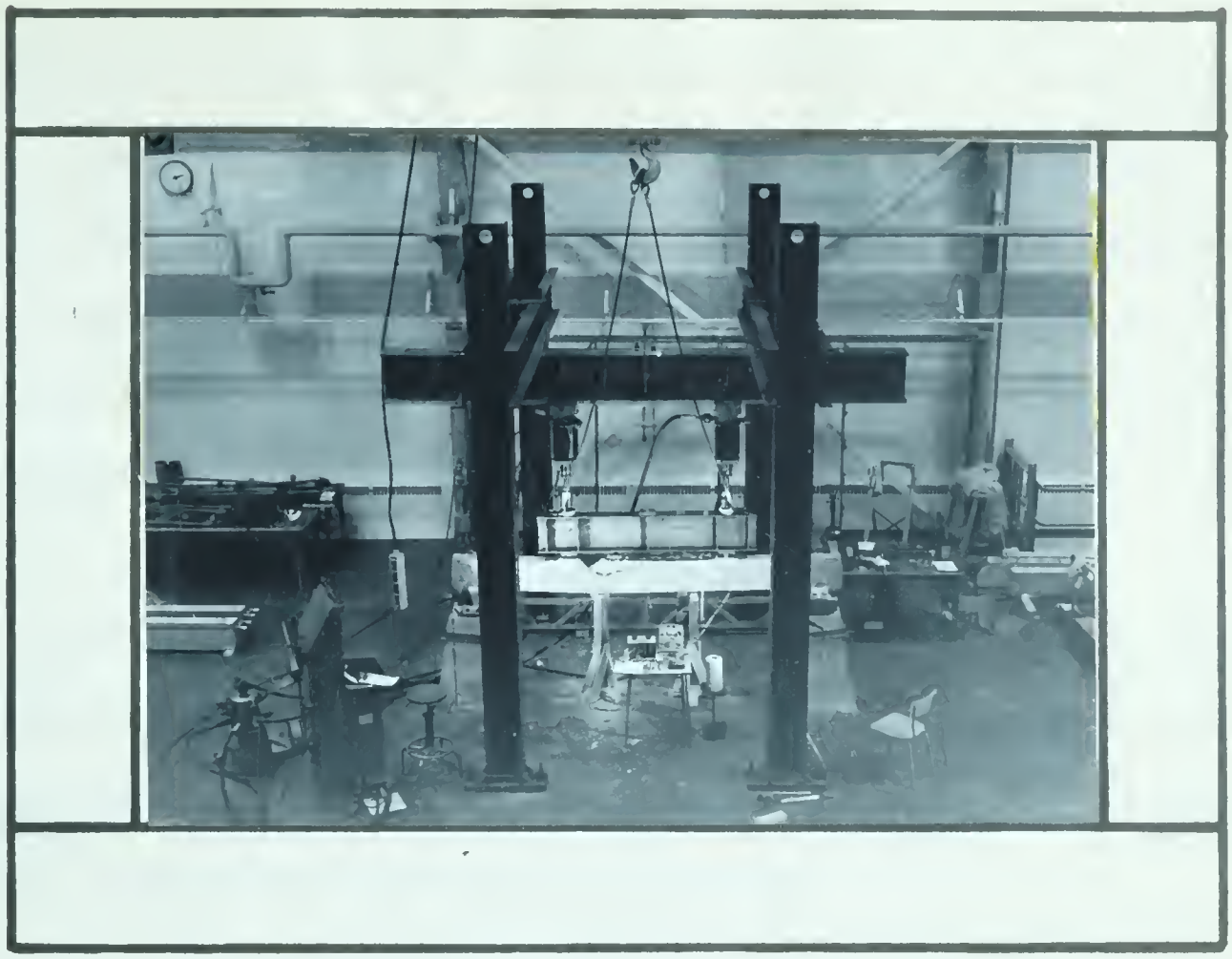

FIGURE 4.7. OVERALL VIEW OF LOADING APPARATUS USING TWO JACKS FOR A TWO-POINT LOADED BEAM

FIGURE 4.8. OVERALL VIEW OF LOADING APPARATUS FOR A ONE-POINT LOADED BEAM

at midspan (Nos. 7 to 10) the jack was applied directly to the test beam through a 4 x 6-in. bearing plate. All plates that were in bearing against the test beam were set in plaster of paris to provide uniform bearing. A single 44-Kip hydraulic jack was used to supply the loading force for all beams except Nos. 3 and 6 which required two 44-kip jacks. The jacks reacted against a heavy loading frame which was bolted to the floor.

4.3.2. I n s t r u m e n t a t i o n. Strains in the concrete at the extreme fibre were measured by means of Type A3, SR-4 electrical strain gages mounted symmetrically about midspan and on the longitudinal center line of the beam at the following spacing:

Beams No. 1 to 6 : 3, 6 and 9 in.

Beams No. 7 and 8 : 3, 6, 9 and 9 in.

Beams No. 9 and 10 : 3, 6 and 6 in.

Preparation of the surface involved grinding with a portable grinder, sanding with medium textured emery cloth, application of a thin coat of Cycleweld as a sealer followed by a final light sanding with the emery cloth. The gages were mounted using a GA-1 Cement Kit in accordance with the procedure recommended by the manufacturer. A Baldwin-Lima-Hamilton strain indicator was used to measure the strains.

The distributions of strain throughout the depth of the beam were obtained by measurements of deformation using an 8-in. Demec Strain gage. The gage lines were set at the following distances from the top of the beam:

Beams No. 1, 2, 4 and 5 : 1, 3, 6 and 10 in.

Beams No. 3, 6, 7, 8, 9 and 10 : 1, 3 1/2, 6 and 10 in.

The number of gage lines at each distance from the top of the beam was the same for any given beam, but varied for different beams as follows:

Beams No. 1 to 6 : 4

Beams No. 7 and 8 : 7

Beams No. 9 and 10 : 5

These were spaced symmetrically about midspan for all beams. The gage lines were established using small center-holed discs 1/4 in. in diameter and 1/16 in. thick. These discs were attached to the beam with sealing wax.

Deflections of the bottom of the beam were measured with 0.001 in. dials attached to a dexion truss by means of magnets. The dials were located at midspan and at 15 and 30 in. to each side for beams No. 1 to 8; at midspan and at 12 in. to each side for beams No. 9 and 10. The dials may be seen in FIGURES 4.8, 5.8 and 5.9.

The oil pressure required for the testing operation was produced by an Amsler Pendulum Dynamometer which also measured the magnitude of the applied load. The oil is supplied to the jack through an inlet valve, which is provided with a delivery regulator, so that for any definite setting of the valve the quantity of oil flowing through per unit of time remains exactly constant, independent of the pressure behind the valve. The quantity of oil can be regulated by an infinitely variable control from zero to a maximum. The pressure prevailing in the loading element (pressure cylinder) acts on a measuring piston and this piston, by means of a suitable linkage, brings a pendulum out of its position of rest. The amplitude of deflection of the pendulum serves to measure the force exerted. The weight of the pendulum is varied to obtain different ranges of force.

No direct measurement of the strain in the reinforcement was made.

4.3.3. T e s t i n g P r o c e d u r e. Initially, zero readings were taken on each strain gage and the deflection dials adjusted to zero. For all beams, except No. 1, it was then necessary to remove the top cables. This involved applying approximately an equivalent amount of load to that exerted on the beam by the cables and then removing the cables by means of a jacking arrangement.

Failure was reached in 8 to 12 load increments which were varied according to the amount the beam deflected. In later stages of loading a large amount of strain was obtained by applying a relatively small amount of load and near failure straining continued even if the load was not increased. All readings were taken after each load increment was applied. Strain readings became impractical to take near failure because of the continued deformation of the beam. Midspan deflections were read at intermediate stages for a more complete load-deflection record.

Also after each load increment, the extension of cracks was marked together with the appropriate load increment number. In order to keep a permanent record of the crack development, photographs were taken during the later stages of loading and at failure.

The duration of a test was between 2 and 3 hours with approximately 15 minutes devoted to loading and recording of strains and deflections at each load increment.

CHAPTER V

PRESENTATION OF RESULTS

5.1. Introductory Remarks

This chapter is devoted to the presentation of results obtained from the measurements of strains and deflections and the corresponding levels of load. The calculations involved the determination of deformation increments by the subtraction of successive readings and the accumulative addition of the increments to determine the strains and deflections at each stage of loading. In addition, a calibration factor was applied to the Demec readings to convert them into strain.

It was desirable to reference the load-deformation curves to the full-cambered position of the beam. This was not possible with the measurements of strains and deflections because of the presence of the top external cables used to control the tension in the top extreme fiber. However, the strains in the concrete produced by the top cables were in the elastic range. Therefore, the behavior of the beam after the cables were removed was not affected. As a result, when the load-deformation curves were plotted, it was possible to extrapolate the curves back until they intersected the negative deformation axis at zero load. This procedure involved little error because the elastic behavior of the concrete resulted in a load-deformation curve which was nearly linear. When the curves were redrawn, they were transferred along the deformation axis so that they began at the origin which then represented the full-cambered position

of the beam.

For convenience to the reader, the designation of the beams is reviewed. The beams were numbered from one to ten with the "high" strength concrete beams preceding the "low" strength concrete beams. The characteristics of each beam is given in TABLE 5-1.

TABLE 5-1. BEAM CHARACTERISTICS

Beam No.	Type of Loading	No. of Strands	Area of Reinf. ($in.^2$)	$p = \frac{As}{bd}$	f'_c (psi)	Relative Concrete Strength	p/f'_c (10-5/psi)
1	2-point	2	.1154	.00193	6560	High	.0294
2	"	4	.2308	.00384	6420	"	.0598
3	"	6	.3462	.00578	7850	"	.0736
4	"	2	.1154	.00193	4800	Low	.0401
5	"	4	.2308	.00384	5210	"	.0737
6	"	6	.3462	.00578	5390	"	.107
7	1-point	4	.2308	.00384	7550	High	.0509
8	"	4	.2308	.00384	5380	Low	.0714
9	"	4	.2308	.00384	6200	High	.0620
10	"	4	.2308	.00384	4280	Low	.0898

5.2. Load-Midspan Deflection Curves

5.2.1. General remarks. The deflection of the bottom of the beams was measured with five dials, 15 in. apart, for the long beams (Nos. 1 to 8) and with three dials, 12 in. apart, for the short beams (Nos. 9 and 10). These dials were placed symmetrically about midspan. FIGURES 5.1 through 5.4 contain the load versus midspan deflection curves for all beams tested.

All of the curves are similar in shape with three distinct stages of behavior evident. The stages are marked by a change in slope of the curve with the slope nearly constant for a given stage. The extent of these stages of behavior depends on the following major variables: amount of reinforcement, concrete strength, level of prestress, the stress-strain relationships of both the concrete and the reinforcement, and span length as indicated by a comparison of the behaviors of the one-point loaded beams.

The first stage of behavior continues until cracking of the concrete occurs. The extent of this stage is dependent almost entirely on the characteristics of the concrete and the amount of prestressing force. In this region of loading the concrete behaves essentially as a homogeneous material with all plane sections remaining plane. Though the behavior of the concrete is considered to be elastic, it deviates from linearity similar to the early part of the stress-strain curve for concrete..

The second stage of behavior continues from initial cracking until the inelastic range of the reinforcement is reached. Although it is difficult to establish from the load-deflection curve, it is likely

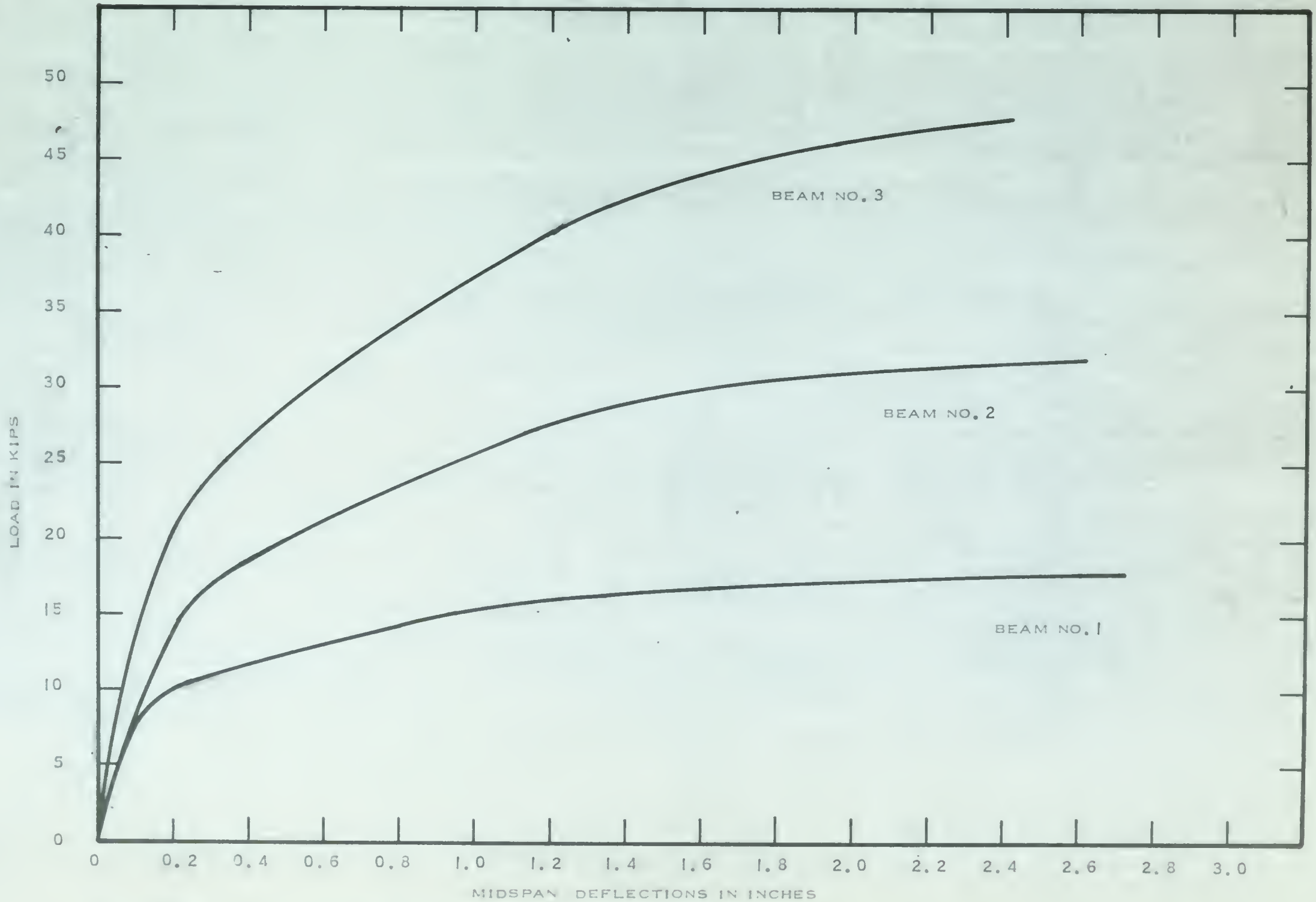

FIGURE 5.1. LOAD-MIDSPAN DEFLECTION CURVES

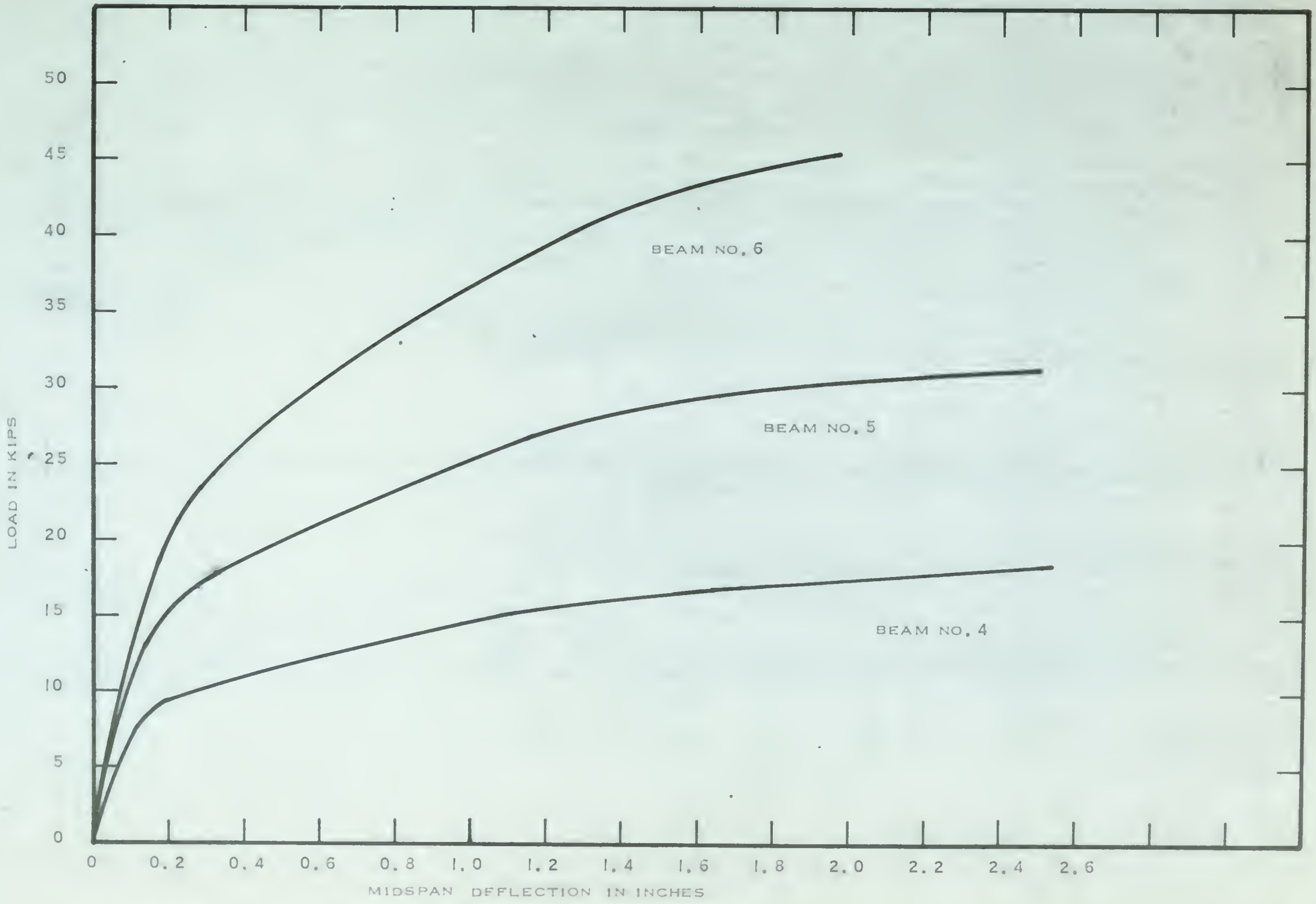

FIGURE 5.2. LOAD-MIDSPAN DEFLECTION CURVES

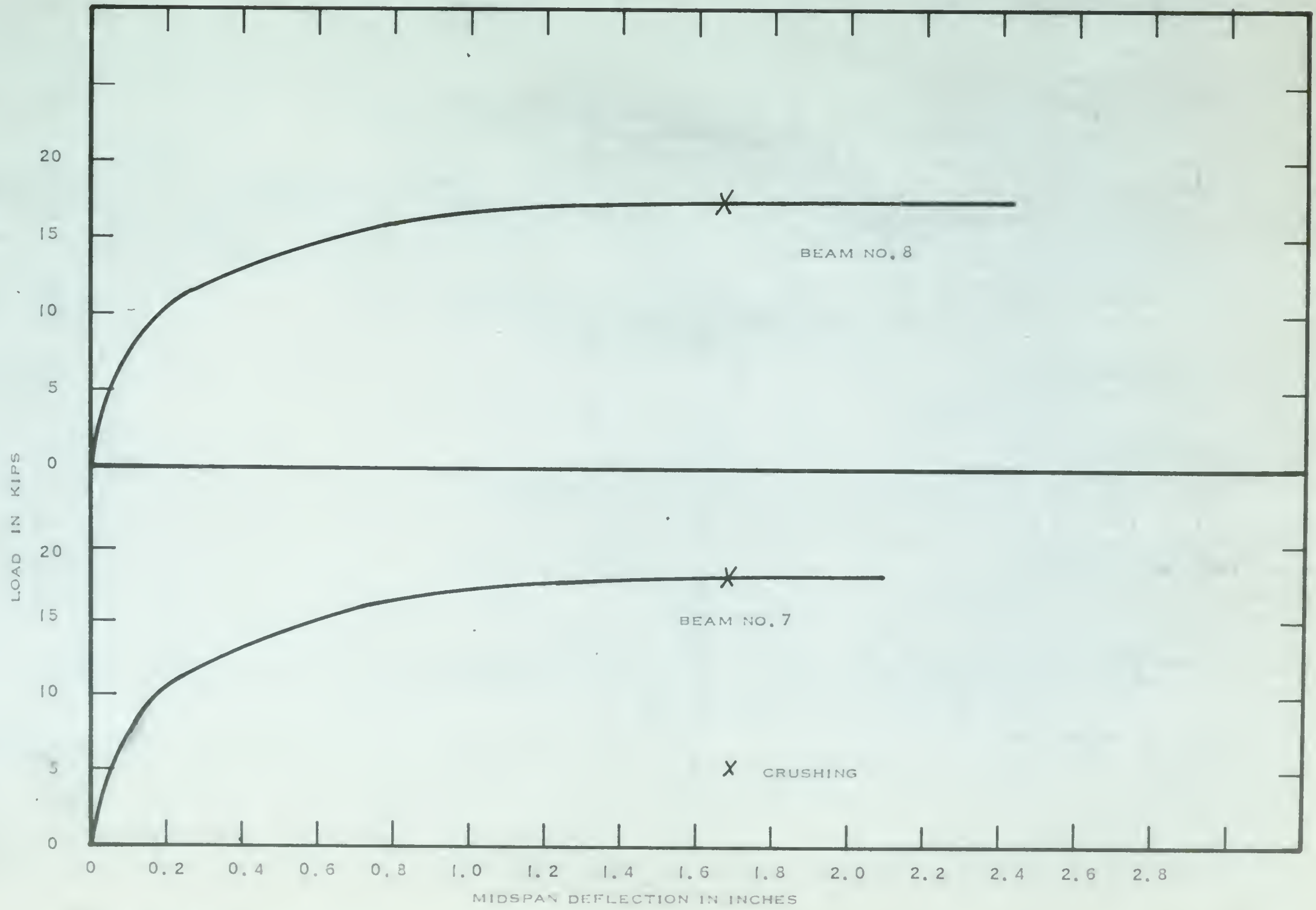

FIGURE 5.3. LOAD-MIDSPAN DEFLECTION CURVES

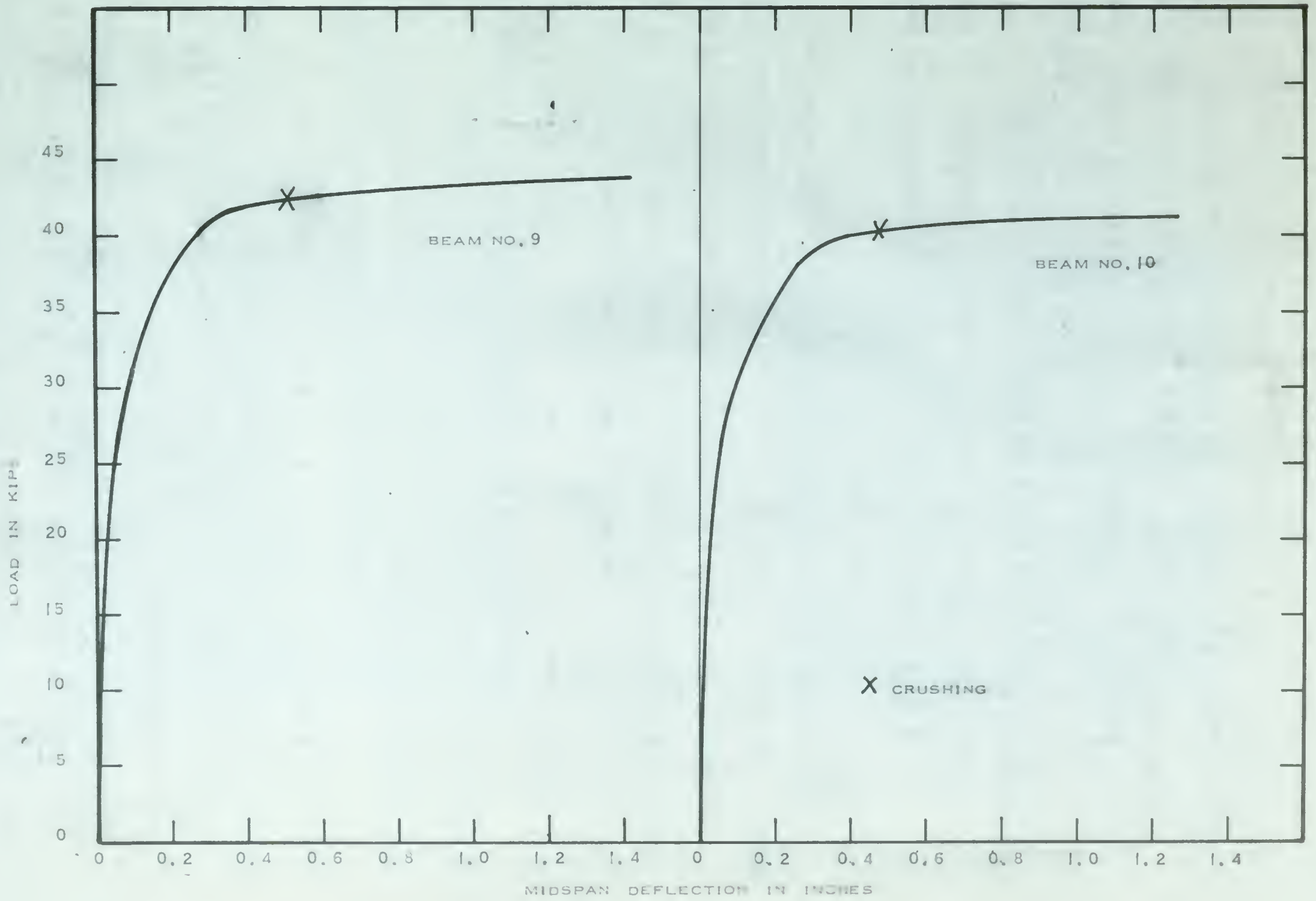

FIGURE 5.4. LOAD-MIDSPAN DEFLECTION CURVES

that in this range the behavior of the compressed concrete changes from what is normally considered elastic to inelastic. The transition from the first stage of behavior to the second stage is generally quite sharp because of the fairly rapid development of cracks which decrease the beam stiffness considerably.

The third and final stage of behavior is marked by inelastic behavior in both the compressed concrete and in the reinforcement. Beams which are heavily reinforced may not exhibit this stage of behavior because the concrete crushes while the reinforcement is still in the elastic range of its stress-strain curve. This stage features large strains and deflections for little increase in load. The cracking becomes quite extensive in the upper regions of the beam. Eventually, the concrete crushes provided that the reinforcement does not fracture. The transition from the second stage of behavior to the third stage is quite gradual. This is probably mainly due to a similar transition in the behavior of the reinforcement from elastic to inelastic.

Photographs which show typical cracking patterns for conditions near failure are presented in FIGURES 5.5 through 5.9. The effects of cracking are discussed in the following sections.

5.2.2. T h e f i r s t s t a g e o f b e h a v i o r. Examination of the load-deflection curves shows that the cracking load is higher for the more heavily reinforced beams. This is a result of the larger prestressing force which produces a more pronounced camber in the beam. This camber must be overcome before the concrete in the lower extreme fiber will crack. The actual effect of the amount of reinforcement is to increase the beam stiffness. However, up to cracking,

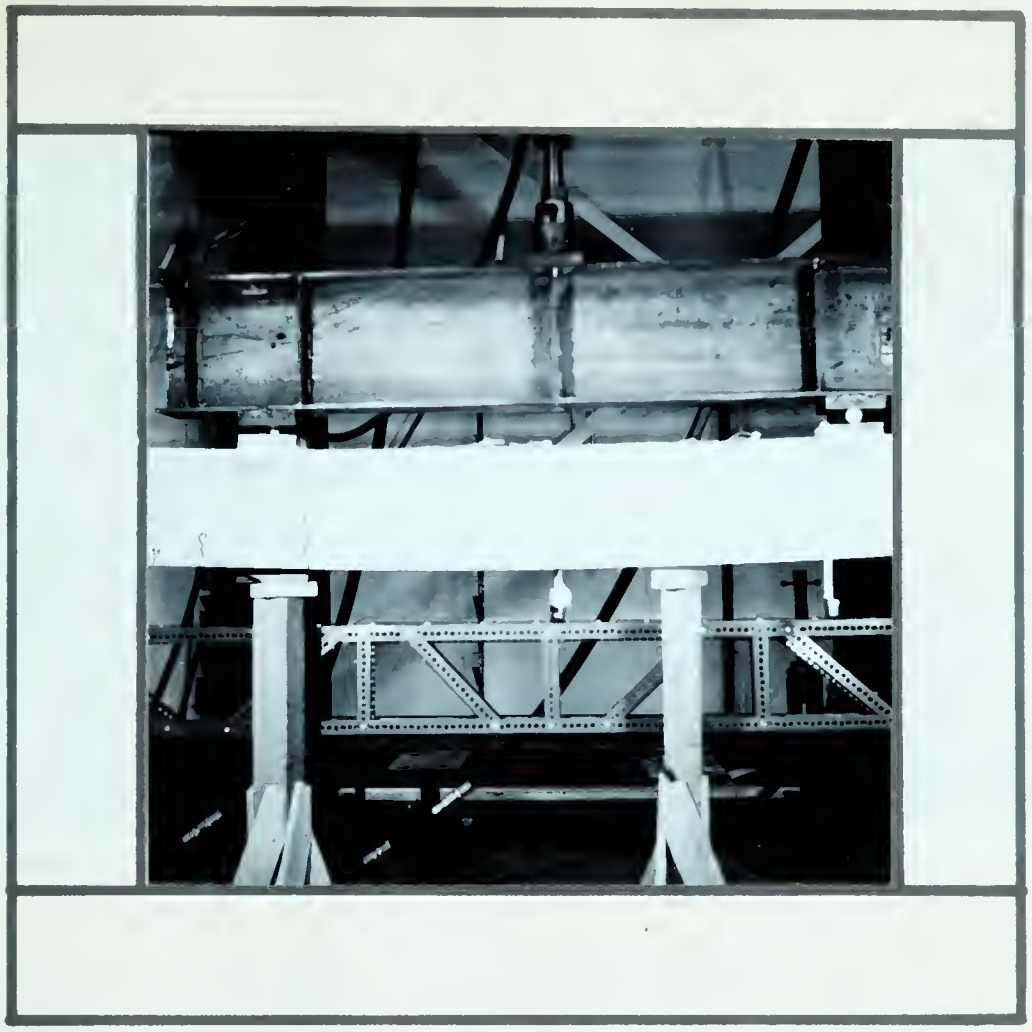

FIGURE 5.5. TYPICAL CRACKING PATTERN FOR A TWO-POINT LOADED BEAM WITH 2 STRANDS

FIGURE 5.6. TYPICAL CRACKING PATTERN FOR A TWO-POINT LOADED BEAM WITH 4 STRANDS

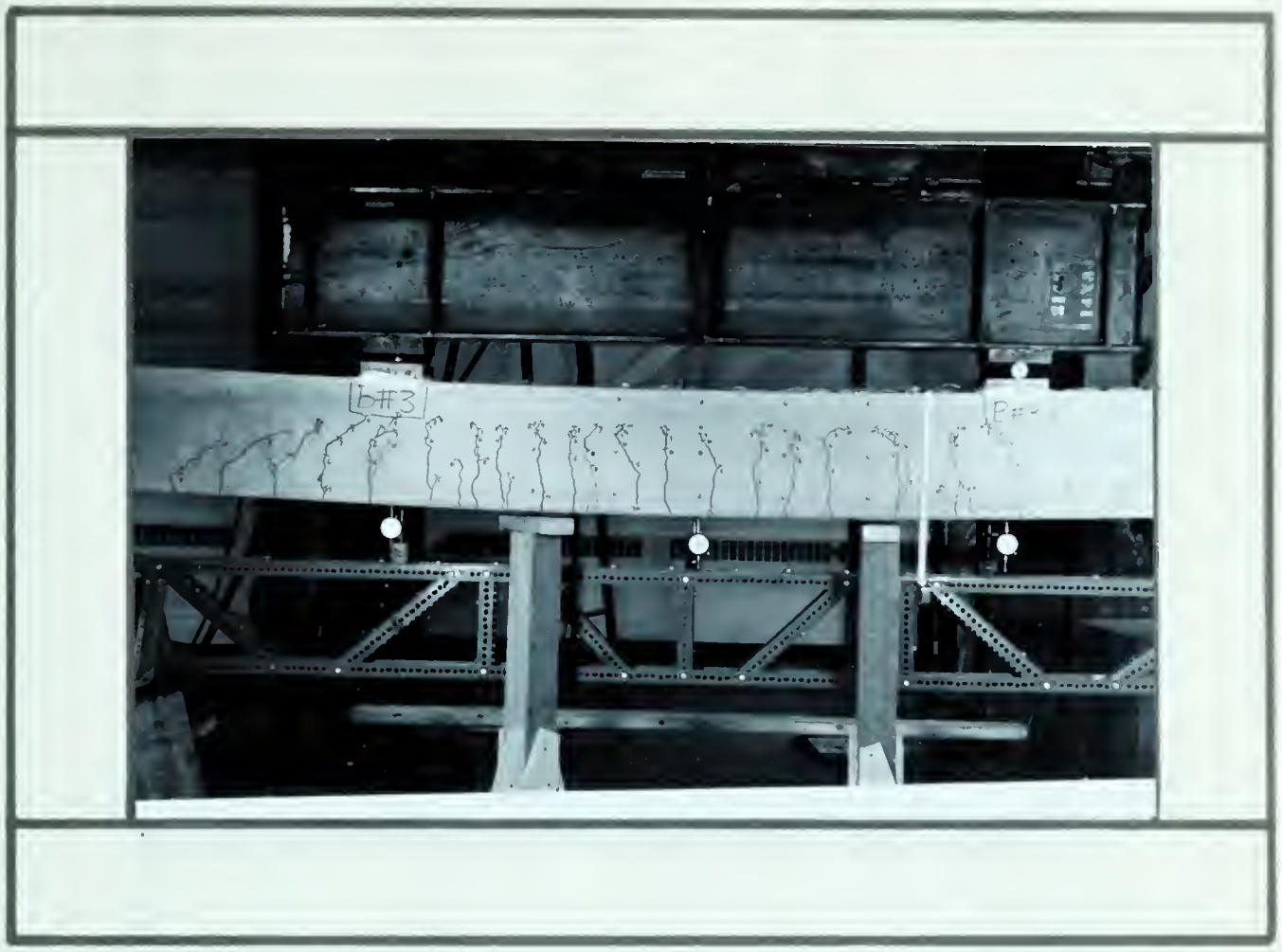

FIGURE 5.7. TYPICAL CRACKING PATTERN FOR A TWO-POINT LOADED BEAM WITH 6 STRANDS

FIGURE 5.8. TYPICAL CRACKING PATTERN FOR A "LONG" ONE-POINT LOADED BEAM

FIGURE 5.9. TYPICAL CRACKING PATTERN FOR A "SHORT" ONE-POINT LOADED BEAM

the entire concrete cross-section is carrying the load. As a result, the amount of reinforcement does not add significantly to the beam stiffness and hence, to the cracking load. Any variation in the initial slopes of the load-deflection curves is almost a direct result of similar variations in the strength of the concrete. Neither the type of loading nor the span length should have any significant bearing over the first stage because the behavior of the beam is governed mainly by the flexural stresses. This is somewhat difficult to confirm from the load-deflection curves because it is not possible to tell exactly where cracking does begin.

5.2.3. The second stage of behavior. The second stage is seen to exhibit a different slope for beams of varying reinforcement ratios. This is due mainly to the smaller beam stiffness in the lower reinforced beams resulting in a greater deflection for a given increment of load. Another effect of the amount of reinforcement is on the spacing of cracks. In the more heavily reinforced beams, the cracks are more closely spaced which reduces strain concentrations resulting in slightly lower deflections. The slope is also increased with the higher strength concrete.

The development of cracks over the second stage is more rapid in the beams with a smaller reinforcement ratio. For a given load the reinforcement strain will be larger in a beam with a small amount of reinforcement than in a similar beam with a larger amount of reinforcement. In addition, the neutral axis will rise much higher in beams with a lower amount of reinforcement because of the large tension strains. There is a tendency for the cracks to branch out during the latter part of this stage.

The load-deflection curves for beams No. 9 and 10 did not exhibit linearity over the second stage of behavior. Since this linearity was common to all other beams, even for beams No. 7 and 8, the difference in behavior cannot be attributed to the type of loading. The cause of this non-linear behavior must be due to the fact that beams No. 9 and 10 were loaded over a relatively short span. Cracking for beams No. 7 and 8 occurred over a wide portion of the beam as contrasted to only three major cracks which occurred in beams No. 9 and 10. In addition, the outside cracks in these latter two beams were inclined at approximately 60 degrees to the horizontal.

An explanation of a possible cause for the non-linearity exhibited by beams No. 9 and 10 could be the following. By considering the equilibrium of the portion of the beam shown in FIGURE 5.10, it is seen that the tension force, T_B, at section B-B is equal to the tension force T_A at section A-A which in turn is equal to the compression force C_A.

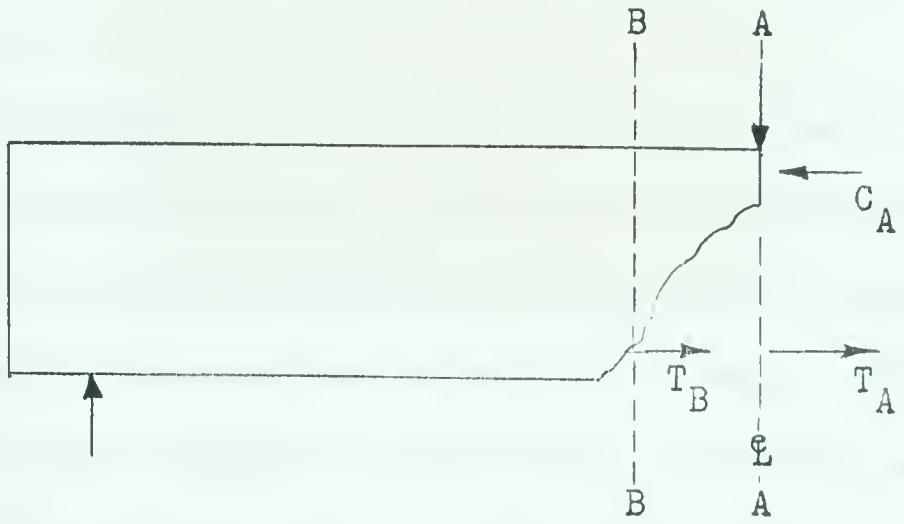

FIGURE 5.10. ELEVATION OF A "SHORT" BEAM LOADED AT MIDSPAN

This means that because of the inclined crack, the strains in the reinforcement between sections A-A and B-B occur over a finite length. This then results in a curvilinear relationship between load and deflection in the second stage of behavior, similar to that obtained for unbonded beams (1). Because this behavior resulted in larger deflections in the second stage, the extent of the third stage of behavior was reduced.

5.2.4. The third stage of behavior. As mentioned previously, the third stage is generally marked by inelastic strains in both the concrete and in the reinforcement. If the reinforcement ratio is large, the strength of the reinforcement will be high compared to that of the concrete. As a result, crushing of the concrete will occur

quite rapidly resulting in a short third stage. If the reinforcement happens to be still elastic, then crushing of the concrete will occur very rapidly without actually reaching the third stage of behavior. However, if the amount of reinforcement is small, then the strengths of the reinforcement and concrete will be of the same order with the result that straining will continue over a wide range with little increase in load.

It may be noted that even though beams No. 3 and 6 exhibited almost no third stage of behavior, the ultimate deflections were still of the same order as the less highly reinforced beams in which a large portion of the deflection occurred in the third stage. This is explained by the fact that with a highly reinforced beam the neutral axis is lower for a given load level than in a similar less highly reinforced beam. Hence, larger curvatures and corresponding deflections are obtained for a lesser amount of strain in the reinforcement. As a result, the reinforcement remains elastic for a greater range of loading. However, the compensating factor is that the concrete compressive strains are much higher and the strains extend over a greater depth of the beam so that when failure occurs, it is generally quite explosive.

The one-point loaded beams deflected considerably after initial crushing occurred. One reason for this behavior is the confining effect of the bearing plate at midspan. Another is that once initial crushing began at one section, it was possible for some of the stresses to be transferred to adjacent sections which were less strained. This was not possible for the two-point loaded beams because the entire central span was subjected to the same moment. It was also possible

that that stirrups were closely enough spaced to confine the concrete and thus increase the rotation capacity of the beam.

5.2.5. Discussion of the use of p/f'_c as a variable. When analyzing the behavior of prestressed concrete beams, it is desirable to have a variable which describes the components making up the cross-section of the beam. An example of such a variable is the reinforcement ratio, p, which is defined as the ratio of the amount of reinforcement to the cross-sectional area given by b x d. Another such variable, p/f'_c, was used extensively in (1). However, with the use of p/f'_c, there arises the problem that the same value of p/f'_c can be obtained from two different beams having the same shape of cross-section. That is, one beam may have a high reinforcement ratio and high concrete strength and the other beam a lower reinforcement ratio and a low concrete strength. When this happens, there is the question of whether these two beams will behave similarly.

Beams No. 3 and 5 had p/f'_c ratios which were almost identical. Dimensionless load-deflection curves are compared for these two beams in FIGURE 5.11. The curve for beam No. 5 falls consistently higher, on the order of 5 to 10 per cent, than the one for beam No. 3. This difference could be due to the fact that the level of prestress was approximately 10 per cent higher for beam No. 5. On the basis of this case the proposed use of p/f'_c as a true variable seems reasonable.

5.3. Distribution of Strains Along Extreme Fiber

The strains along the top of each beam were measured with Type A-3, SR-4 strain gages which had a 3/4 in. gage length. Typical distributions of strain over the flexure span for the two-point loaded beams are shown in FIGURES 5.12 through 5.14 along with the corresponding crack patterns at failure. These are given for various stages of loading. Similarly, a typical series of strain distributions for a one-point loaded beam is shown in FIGURE 5.15. The average strain for the last load increment recorded is shown in all cases. It compared favorably with the average from the Demec gages, which is also given.

The strains over the span of pure flexure were not uniform for any beam. Variations were the result of strain concentrations caused by cracking. Because of the random fashion of cracking with respect to the location of the SR-4 gages, it is difficult to hypothesize the effect a crack might have on the reading of a gage. However, in most instances a major crack will be found to occur directly under a peak in the strain distribution. Once the location of the cracks at the bottom of the beam was established the strain distribution assumed a particular shape which it maintained throughout the entire sequence loading: similarly, no new major cracks developed in the flexure span once the initial crack pattern developed. This indicates that the non-uniformity in the strain distribution is caused by cracking. Another verification is that the strain distributions were more uniform for the more heavily reinforced beams in which the cracks were more closely spaced tending to reduce the strain concentrations.

All the one-point loaded beams showed a marked concentration

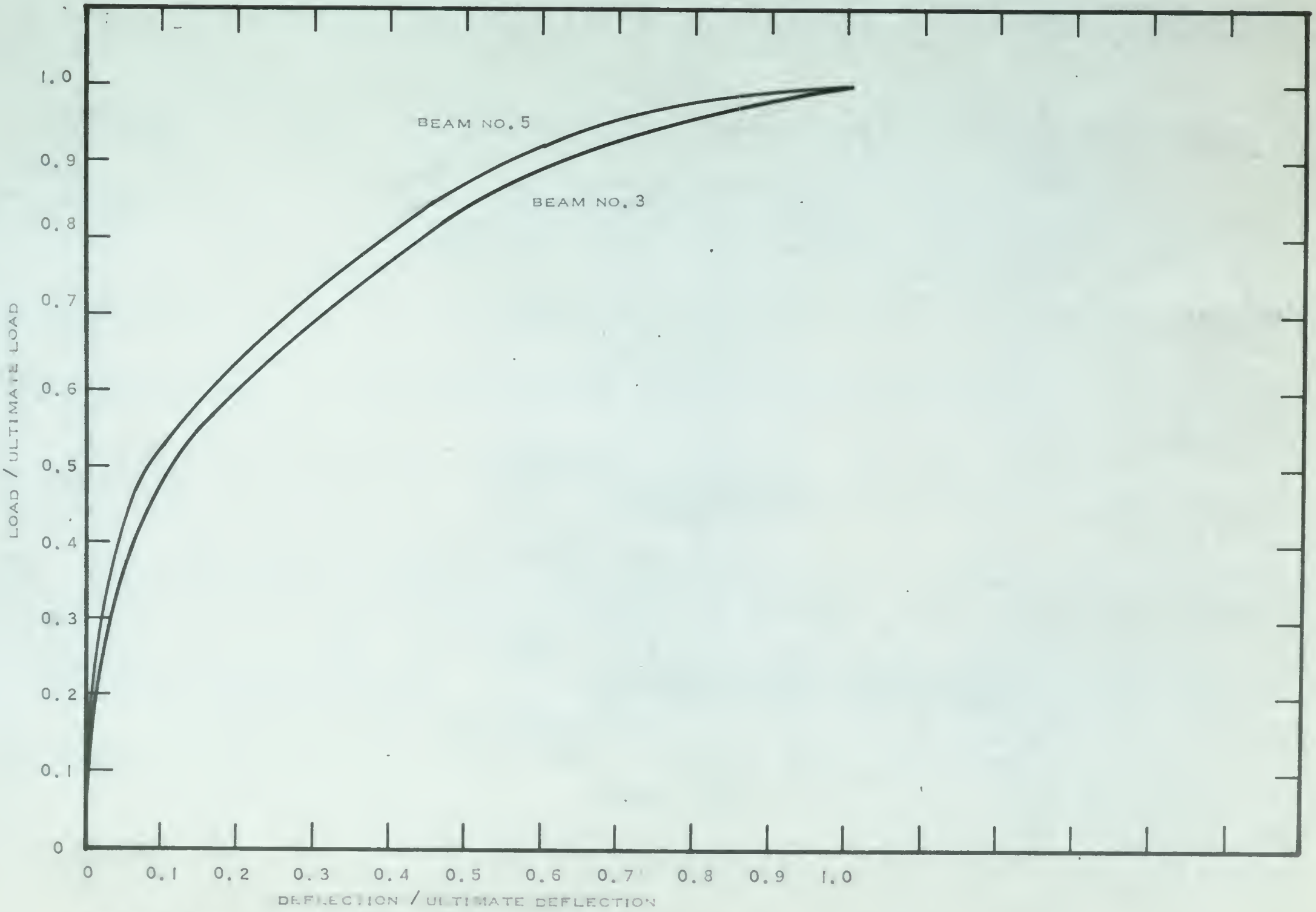

FIGURE 5.11. DIMENSIONLESS LOAD-MIDSPAN DEFLECTION CURVES

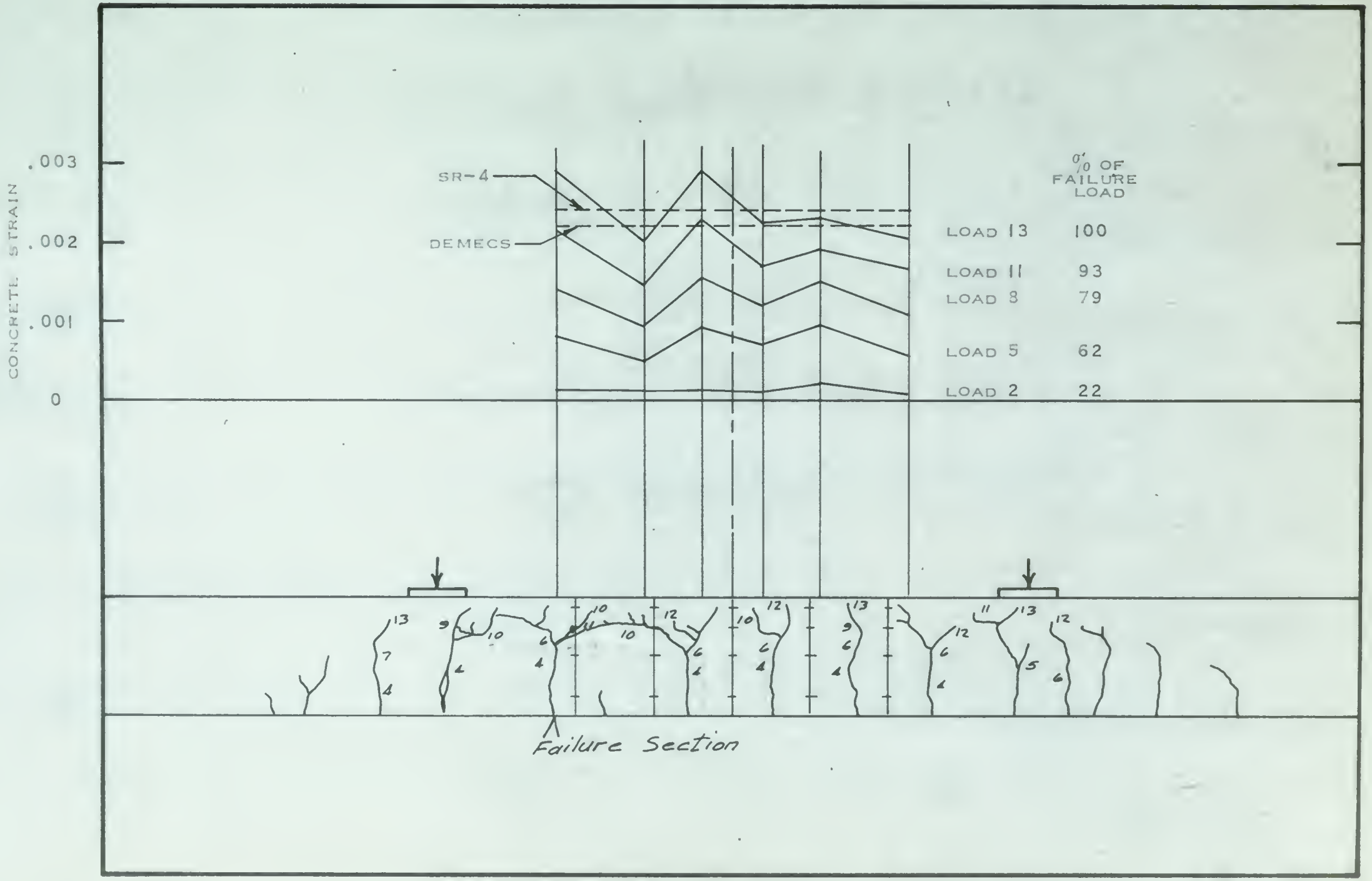

FIGURE 5.12. DISTRIBUTIONS OF STRAINS ALONG THE TOP OF BEAM NO. 1 AND THE CRACK PATTERN AT FAILURE

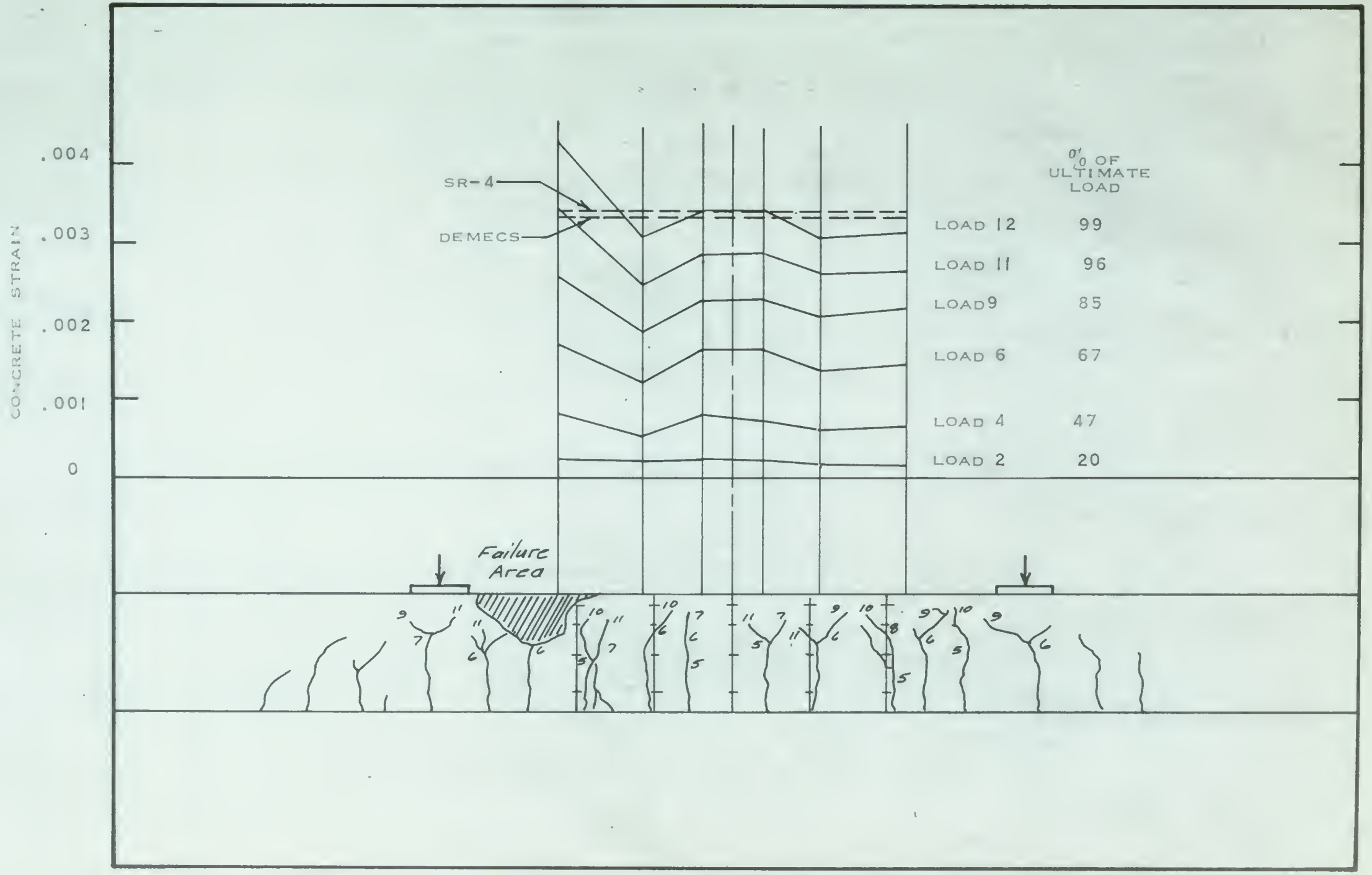

FIGURE 5.13. DISTRIBUTIONS OF STRAINS ALONG THE TOP OF BEAM NO. 2 AND THE CRACK PATTERN AT FAILURE

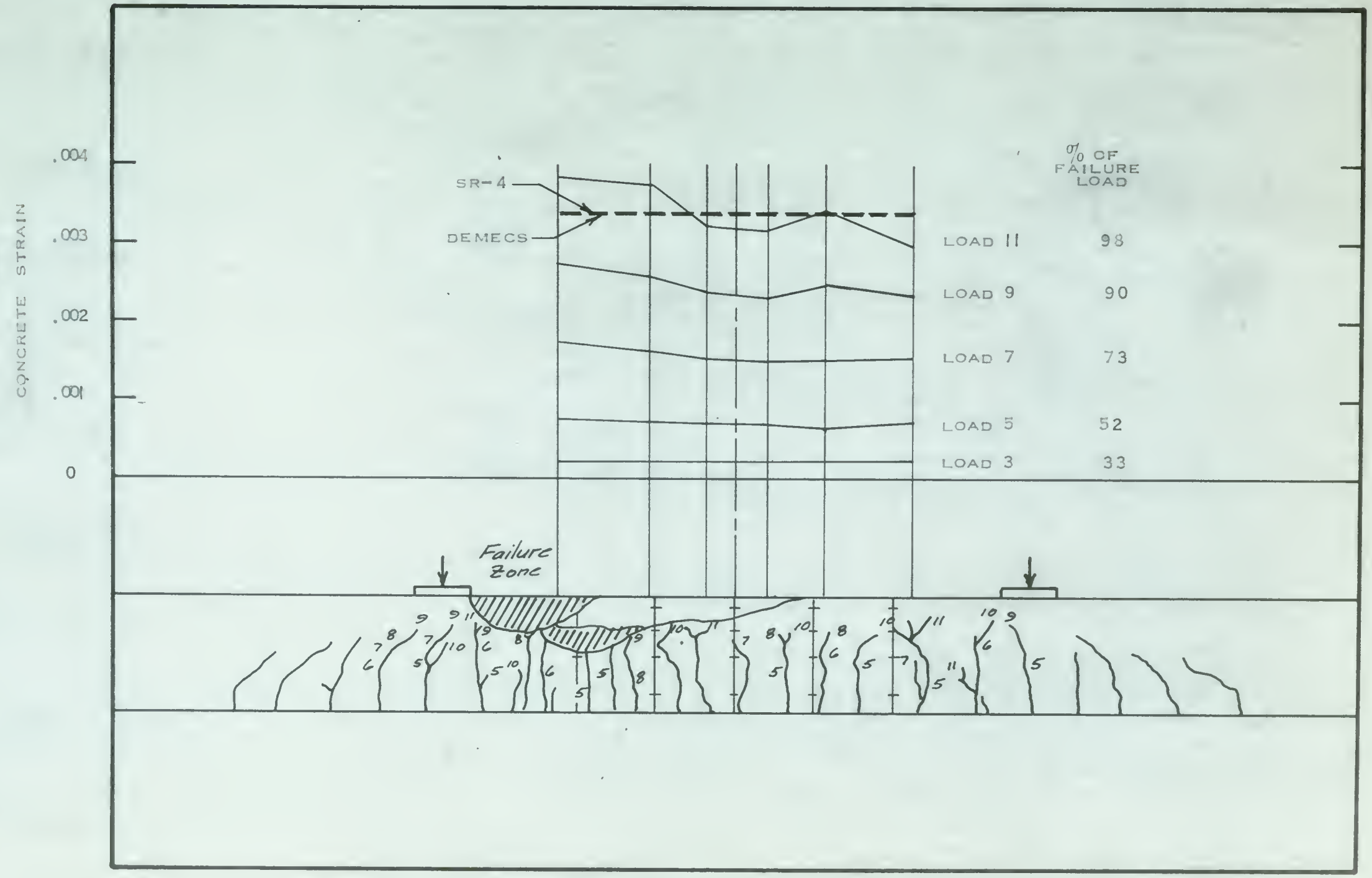

FIGURE 5.14. DISTRIBUTIONS OF STRAINS ALONG THE TOP OF BEAM NO. 3 AND THE CRACK PATTERN AT FAILURE

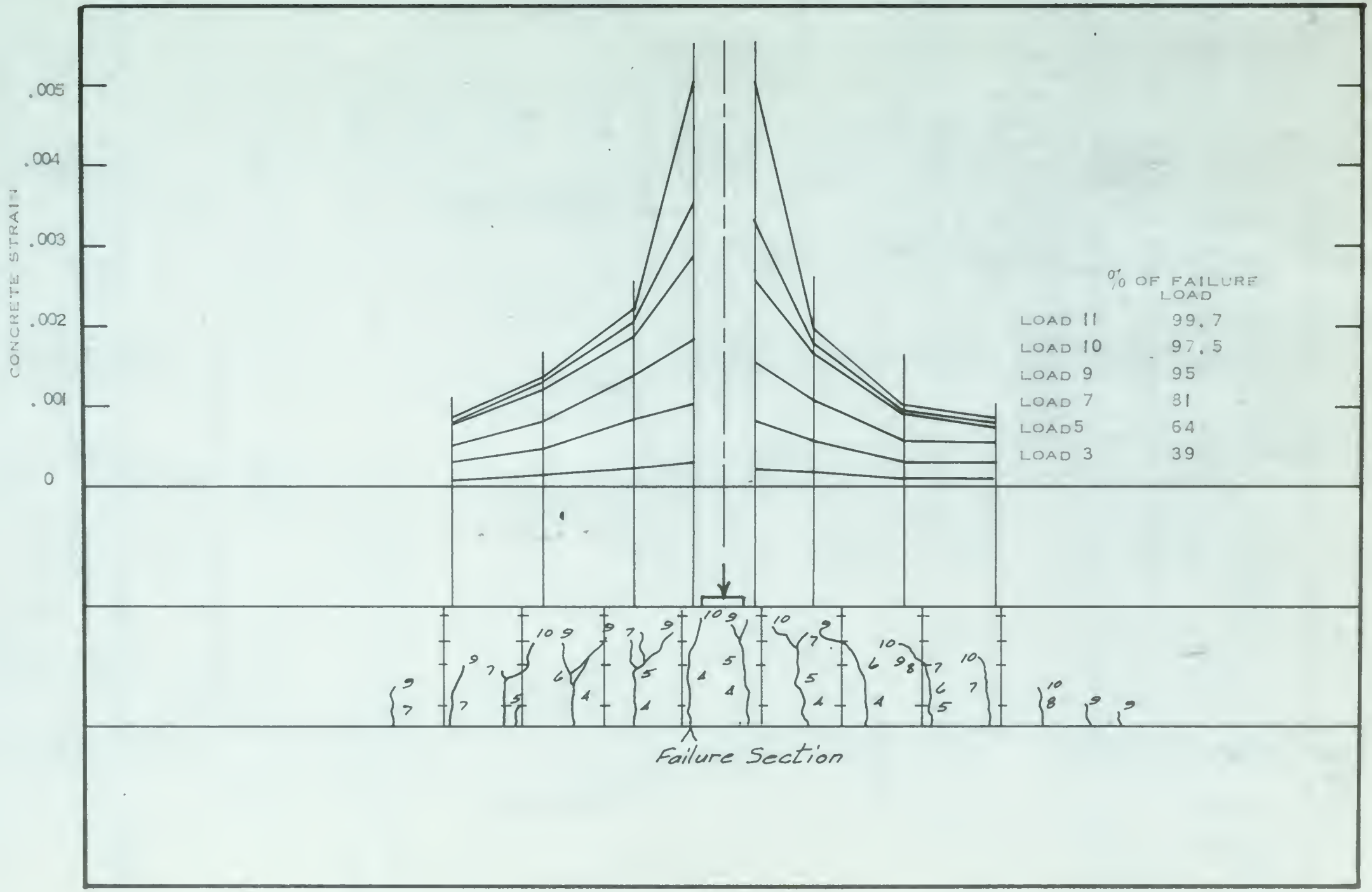

FIGURE 5.15. DISTRIBUTIONS OF STRAINS ALONG THE TOP OF BEAM NO. 7 AND THE CRACK PATTERN AT FAILURE.

of strain in the central region of the beam, especially near failure. This concentration of strain was mainly the result of the type of loading which features a "peaked" bending moment-diagram. With this type of loading, the maximum strains occur at midspan even in the elastic range. Once these strains are aggravated by cracking, they can become very large in the central region of the beam.

FIGURE 5.16 shows a plot of limiting concrete strain, ϵ_u, versus concrete strength using the results from the two-point loaded beams. It shows that 0.004, which was the value assumed in (1) is reasonable.

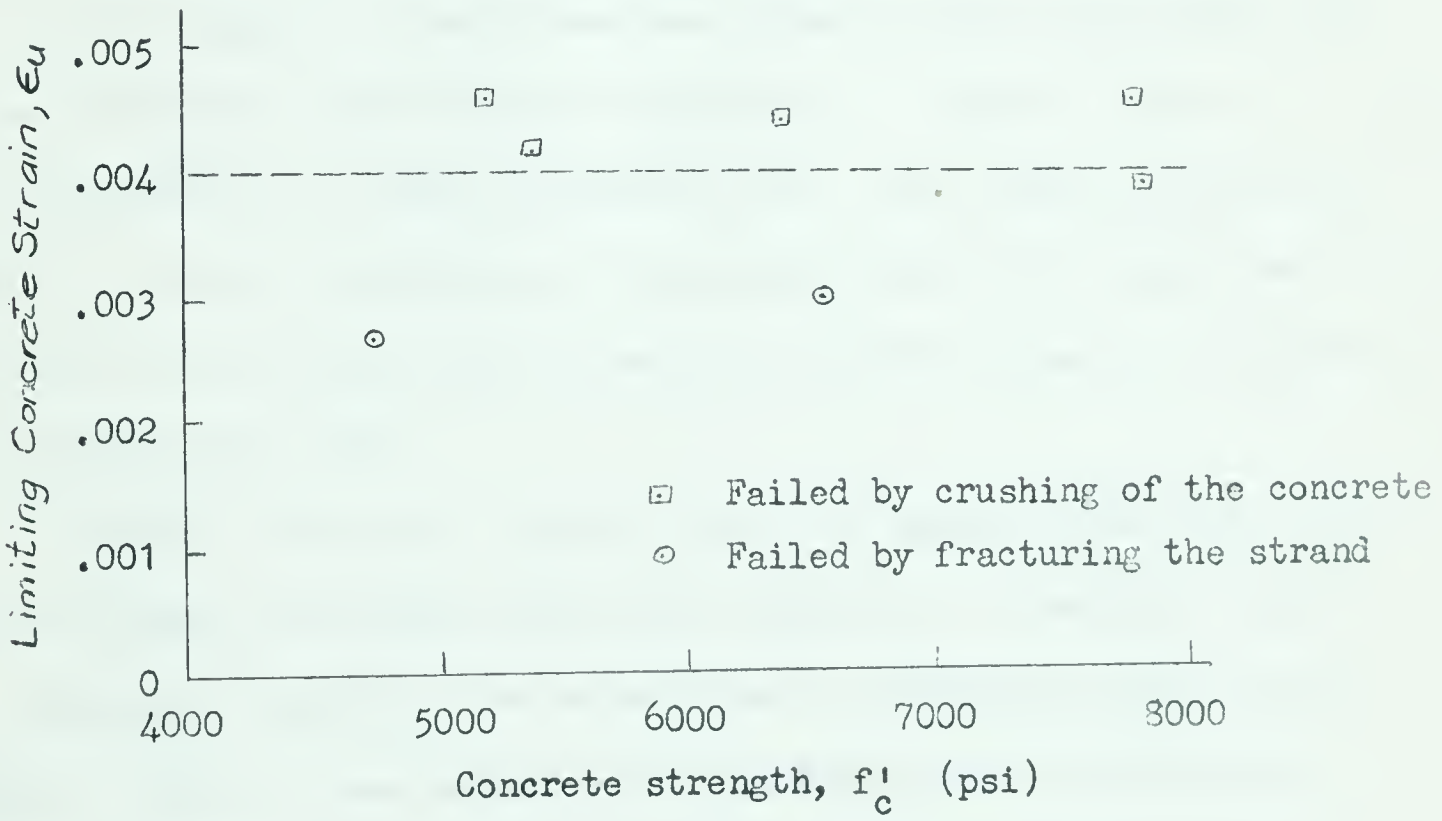

FIGURE 5.16. RELATIONSHIP BETWEEN LIMITING CONCRETE STRAIN AT FAILURE AND COMPRESSIVE CONCRETE STRENGTH

5.4. Distribution of Strains Over Depth of Beams

Strains over the depth of the beams were measured with an 8-in. Demec gage. During the early stages of loading each individual column of gages showed a linear distribution of strain. However, once cracking developed these distributions became quite erratic. With cracks between the Demec points, the strains measured were no longer those in the concrete, but were in most part a measurement of the opening of the cracks.

In spite of the lack of linearity in the strain distributions measured on the various sets of gage lines, an average distribution for the central half of the flexure span of two-point loaded beams based on four readings at each level was linear in all cases except for two load increments near failure in beam No. 2. A typical series of strain distributions is shown in FIGURE 5.17. Thus, when the "average" behavior of a beam is considered, Bernouilli's theory that plane sections remain plane after bending may be assumed to be true, even up to failure, without appreciable error.

FIGURE 5.18 shows a typical series of strain distribution from one set of gage lines symmetrical about midspan for a one-point loaded beam. Because of cracking, the actual strain distributions were quite irregular. Hence, it was necessary to approximate the distributions with a straight line in order to be able to compute moment-curvature relationships which are presented in CHAPTER VI. After attempting a number of possibilities, as to where to draw the line, it was concluded that the only method which would give reasonable results and at the same time be used consistently for all one-point loaded beams was to pass the straight line through the point in the compression zone and at an average

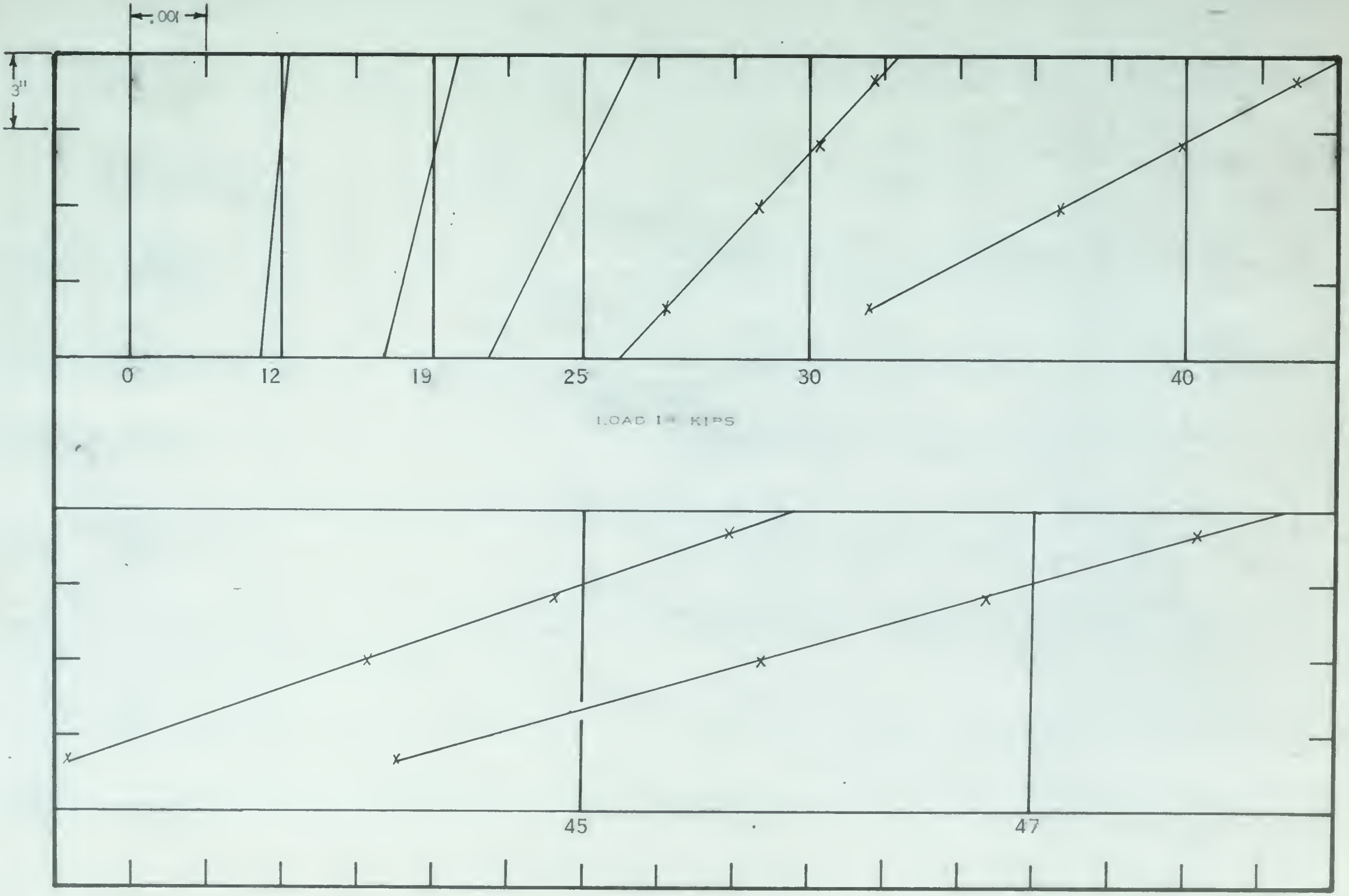

FIGURE 5.17. DISTRIBUTIONS OF STRAIN OVER THE DEPTH OF BEAM NO. 3

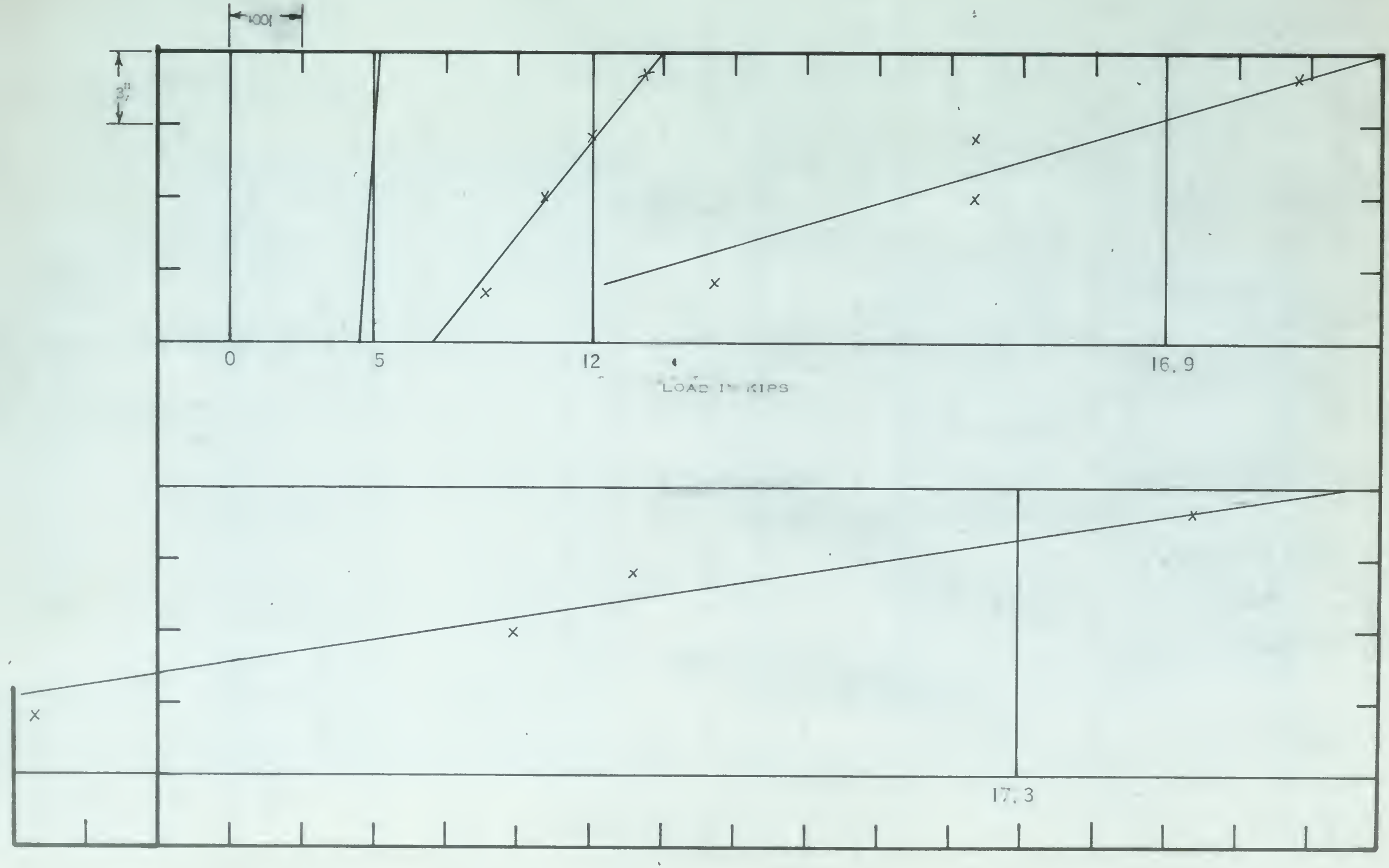

FIGURE 5.18. DISTRIBUTIONS OF STRAIN OVER THE DEPTH OF BEAM NO. 8

distance between the other points. Reasonable correlation of strains along the top of each beam with the SR-4 gages was obtained from the method.

5.5. Types of Failure

Both compression and tension failures were obtained. Photographs of the typical types of failure are shown in FIGURES 5.19 through 5.22. Of the two-point loaded beams, Nos. 1 and 4 failed by fracturing of the cables indicating a very under-reinforced beam. Beam No. 2 failed by a gentle crushing of the concrete. The strains at beam failure in the reinforcement, as indicated by the strains over the gage lines at the level of the reinforcement, were of the same order as those obtained in beams No. 1 and 4 indicating that the strand was near fracture. The compressed concrete in beams No. 3, 5 and 6 failed in quite an explosive manner which is characteristic of an over-reinforced beam.

All the one-point loaded beams failed ultimately by fracturing of the strand though crushing had occurred previously. It was noted that there was a stirrup at each of the failure sections. This probably did not affect the capacity of the beams, but had some influence on the pattern of crack development.

No indication of crushing was observed in the beams loaded at two points until just before failure occurred. This rapid type of failure is probably due to the very high tension in the reinforcement and to the fact that a considerable length of the beam is subjected to the same moment.

FIGURE 5.19. TYPICAL FAILURE OF A TWO-POINT LOADED BEAM BY FRACTURING OF THE STRAND

FIGURE 5.20. TYPICAL FAILURE OF A TWO-POINT LOADED BEAM BY GENTLE CRUSHING OF THE CONCRETE

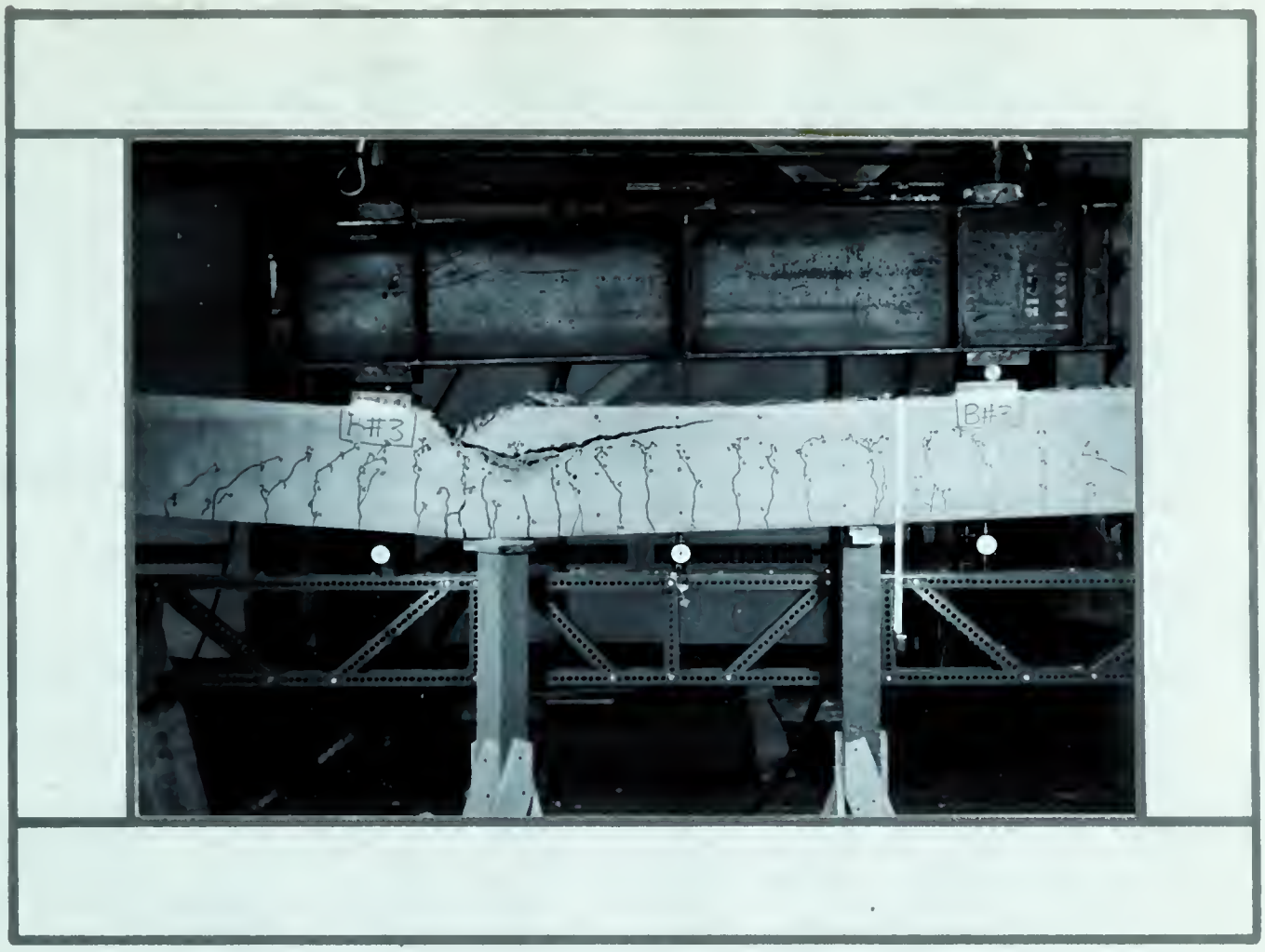

FIGURE 5.21. TYPICAL FAILURE OF A TWO-POINT LOADED BEAM BY EXPLOSIVE CRUSHING OF THE CONCRETE

FIGURE 5.22. TYPICAL FAILURE OF A ONE-POINT LOADED BEAM BY FRACTURING OF THE STRAND

CHAPTER VI

DERIVATION OF MOMENT-CURVATURES FROM RESULTS

6.1. Introductory Remarks

In this chapter, the strains and deflections presented in the previous chapter are used to determine moment-curvature relationships. Once the moment-curvature relationship is known, it is a matter of simple geometry to obtain the load-deflection curve which is of major concern in structural design.

6.2. Computation of Moment-Curvatures from Deflection

6.2.1. Two-point loaded beams. For the beams loaded at two points symmetrical about midspan, the central span was subjected to pure moment. Theoretically, this span had a constant curvature, i.e. it formed the arc of a circle. The deflection of these beams was measured at five points spaced symmetrically about midspan and located on the longitudinal centerline of the beam.

In determining the curvature, the deflections from each pair of dials, symmetrical about midspan, was averaged. Each of the two average deflections was subtracted from the midspan deflection resulting in three ordinates which defined the deflected shape of the beam. Since only two ordinates were required to define a circle, two circles were determined from the three ordinates. One circle was passed through the origin and one of the other points; the other passed through the origin

and the remaining point. The curvature was then obtained by taking the reciprocal of the average radius of the two circles. This procedure was followed for each load increment and the resulting moment-curvatures are shown in FIGURES 6.1 and 6.2.

6.2.2. One-point loaded beams. The problem of determining moment-curvatures for the beams loaded only at midspan was more complicated because of the presence of shear. As for the two-point loaded beams, corresponding deflections symmetrical about midspan were averaged and then the average deflections were subtracted from the midspan deflection. For beams No. 7 and 8 a third degree polynomial was passed through the three points. The polynomial was determined on the basis that the rate of change of curvature is constant over the length of the beam and by solving for the constants of integration from the deflection ordinates. The relationships between the moments and corresponding curvatures, which were obtained using this procedure, are shown in FIGURE 6.3.

Since only three dials were used to measure the deflection of the short beams, a polynomial of the second degree had to be assumed to represent the deflected shape of the beam. A parabola was chosen on the basis that it gave a reasonable indication of the behavior of the beam as compared to that observed during the tests. The relationships between the moments and corresponding curvatures, which were obtained using this method, are shown in FIGURE 6.4.

6.2.3. Discussion of procedures used for determining curvatures. There is little theoretical justification for the use of the third degree polynomial and the parabola in determining the curvatures. Though the derivation of the

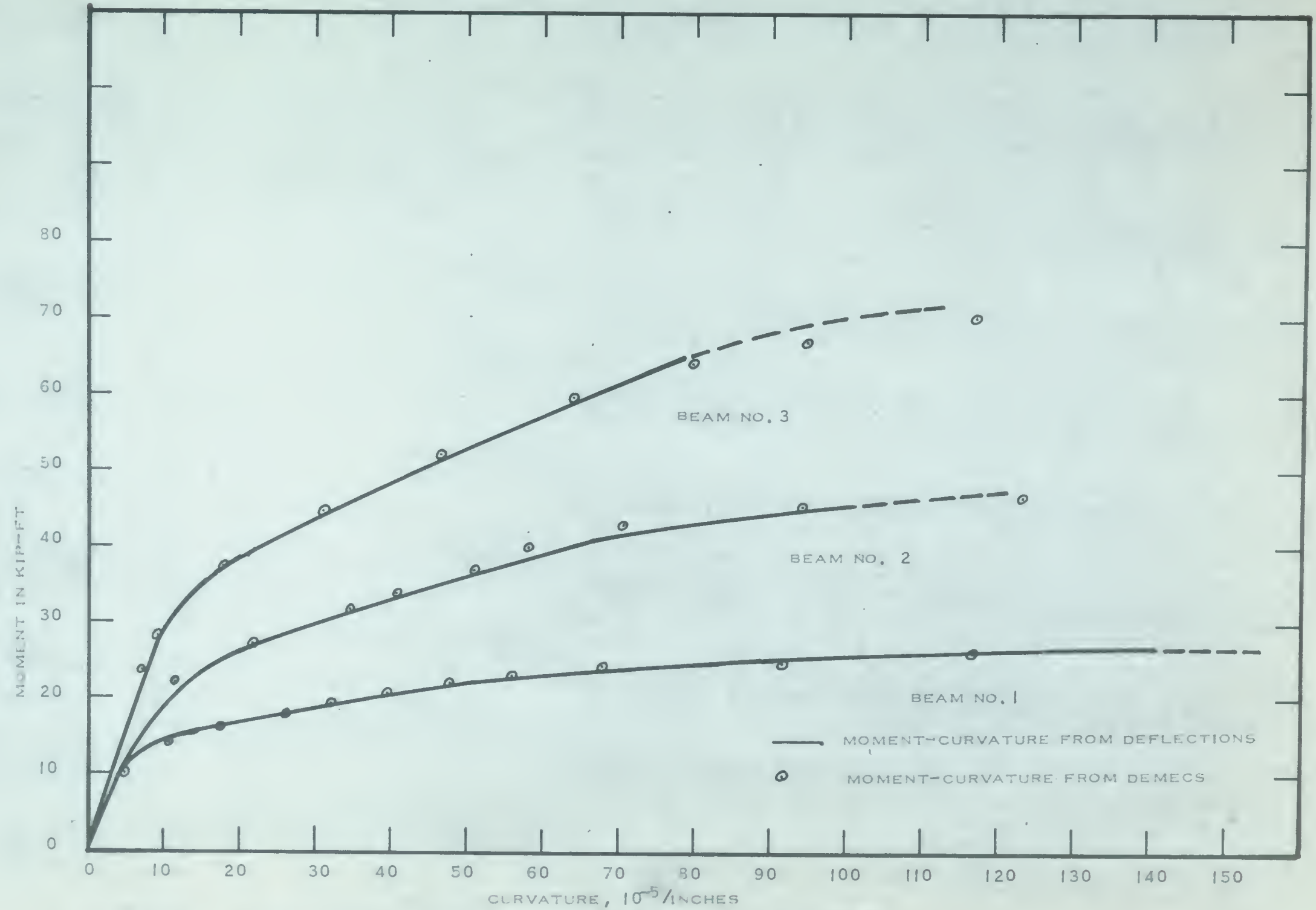

FIGURE 6.1. MEASURED MOMENT-CURVATURE RELATIONSHIPS

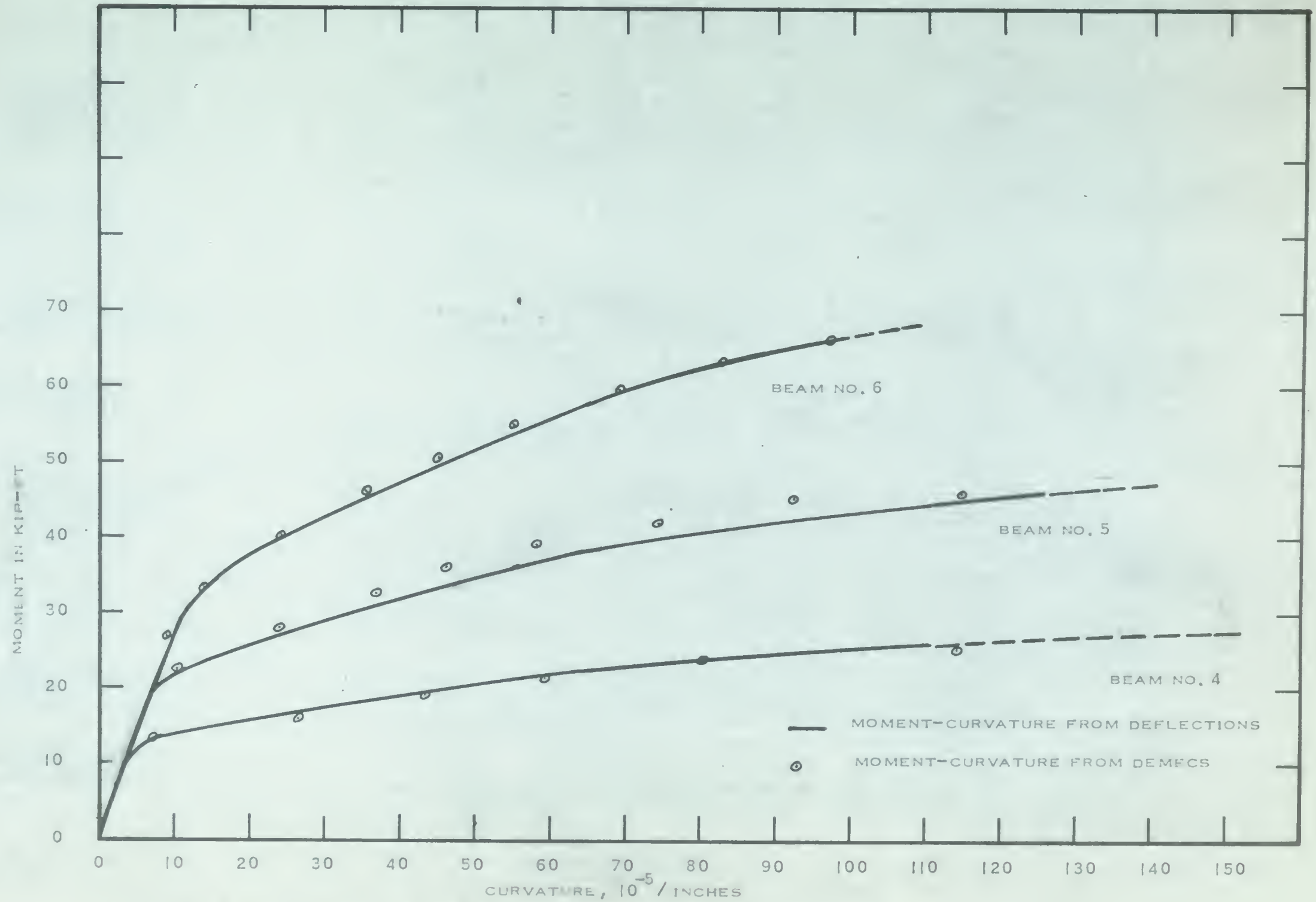

FIGURE 6.2. MEASURED MOMENT-CURVATURE RELATIONSHIPS

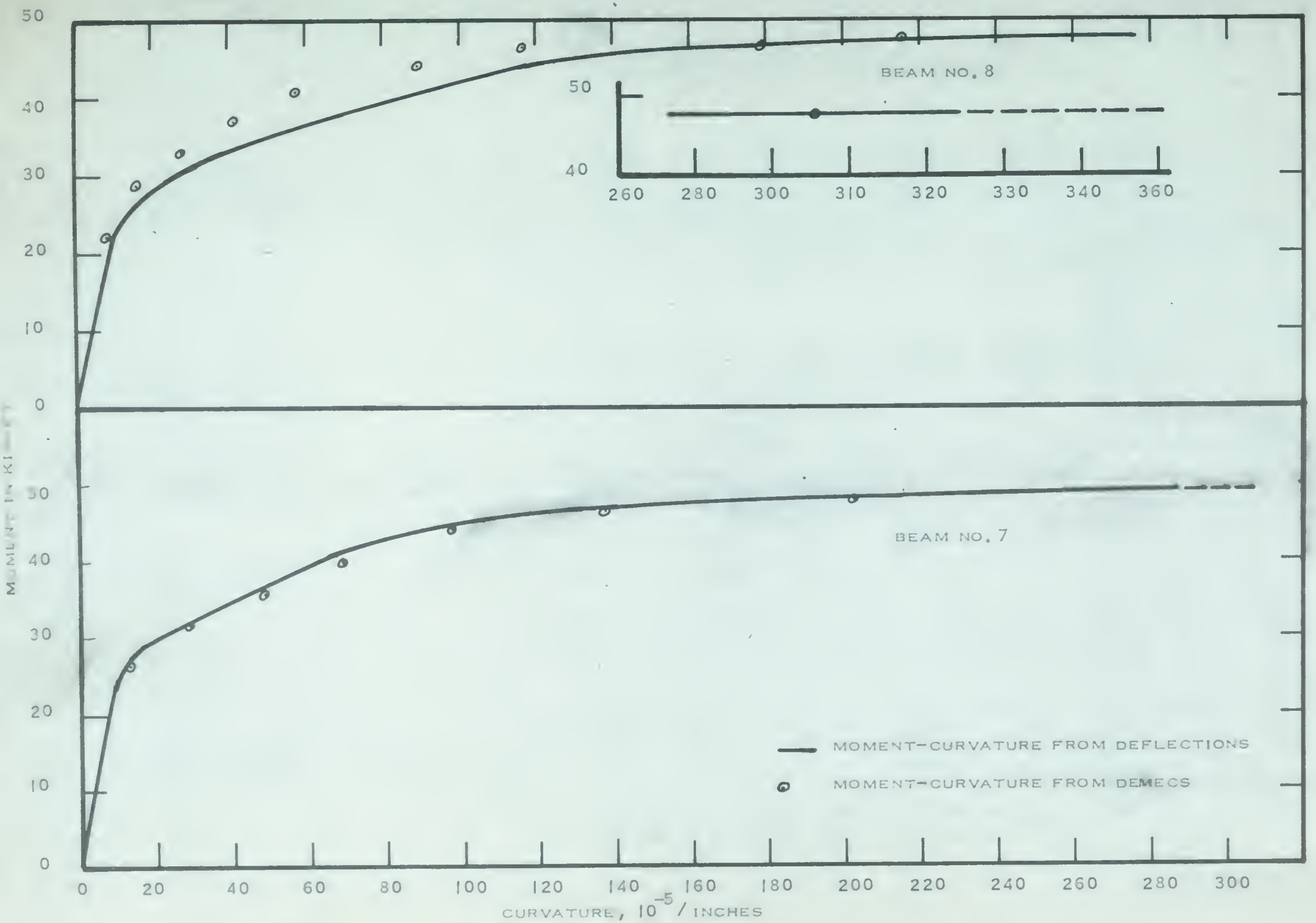

FIGURE 6.3. MEASURED MOMENT-CURVATURE RELATIONSHIPS

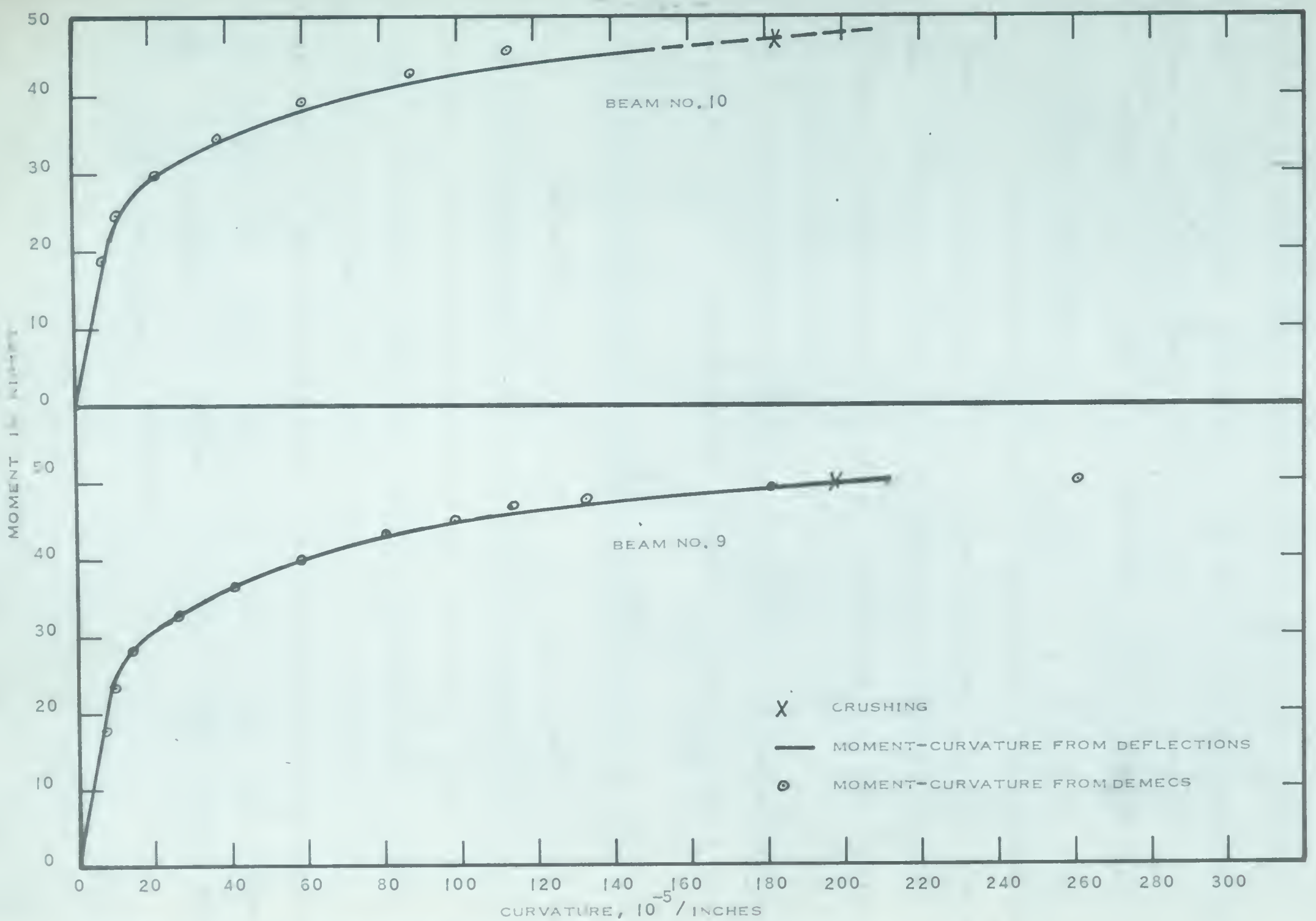

FIGURE 6.4. MEASURED MOMENT-CURVATURE RELATIONSHIPS

former curve was based on elastic theory, the use of a third degree curve allows reverse curvature to occur in order that the curve fit all the points. Reverse curvatures were obtained near the outside coordinates. However, a reasonable shape of the curve was obtained in the immediate vicinity of midspan. The choice of the parabola had no theoretical basis. The justification for the use of these curves is that they gave results which correlated well with those obtained from the Demec gages and with those theoretically derived.

It should be noted that these curves were used to obtain the curvature at midspan only. That is, once the equation for the curvature was determined, it could be used to solve for the curvature only at midspan. Solving for the curvature at other points away from midspan would lead to serious error.

The procedures followed to determine the curvature from the assumed deflected shape are given in Appendix A for all beams.

6.3. Computation of Moment-Curvatures from Demec Gages

Each of the two-point loaded beams had four sets of gage lines over the constant moment span. When the four readings at each level were averaged, a strain distribution which was very close to linear over the depth of the beam was obtained. These average strain distributions were plotted on graph paper and the curvatures were determined by dividing the strain in the extreme concrete fibre in compression by the depth to the neutral axis. This procedure was followed for each load increment. The resulting moment-curvatures were compared with those obtained from the measured deflections in FIGURES 6.1 and 6.2.

Diffulty in determining the curvatures for the one-point loaded beams arose because of the lack of a constant moment span over which readings could be averaged. It was decided to use only the middle set of gage lines and to assume a straight line distribution as was explained in Section 5.4. An alternate procedure would be to average the readings of the middle set of gages with the two adjacent sets. However, because of the decrease in curvature away from midspan, as a result of the type of loading, the resulting curvatures would be on the low side. This method would probably be satisfactory, though somewhat unconservative, for the "long" beams, but unrealistic for the "short" beams because of the high concentration of strain in the immediate region of midspan. Once the assumption was made as to the distribution of strain, the computation of moment-curvatures followed as for the two-point loaded beams. These are shown in FIGURES 6.3 and 6.4 in a comparison with the moment-curvature relationships determined from the deflections.

6.4. Comparison of Experimentally Derived Moment-Curvature Relationships

An examination of FIGURES 6.1 through 6.4 shows that the correlation between the two methods of determining moment-curvature relationships from the measured strains and deflections was good for all beams. However, for beams No. 5 and 8 the Demec gages gave a somewhat higher moment-curvature diagram. Such discrepancies could be the result of assuming the wrong deflected shape, errors in measurement, or the difference in the length of beam covered by the Demec gages and the dials.

For beam No. 8 the discrepancy could be due to the use of the third degree polynomial to obtain the curvatures from the deflections or

due to having only one set of gage lines to determine curvature from the Demec gages. For beam No. 5, the Demec gages measured the strains over 32 in. of the span while the deflection dials were spaced over the entire 5-ft. constant moment span. Hence, if more straining occurred in the outer region of the middle span than in the inner part covered by the strain gages, curvatures computed from the deflections would be higher than those from the Demecs. The fact that the same discrepancies were not prevalent for all beams of the same type, i.e. two-point loaded or one-point loaded, arises from the random spacing of cracks with respect to the position of the Demec points. The discrepancies between curvatures obtained from the deflections and the Demec gages should decrease as the reinforcement ratio increases because as the cracks become more closely spaced, the location of individual cracks has less bearing on the strain over any given gage line.

6.5. Concluding Remarks

It was desirable to have measured strains and deflections for determining curvatures for loads up to failure. However, near failure only midspan deflection and load were recorded. Because of the similarity between the load-midspan deflection curves and the moment-curvature diagrams, it was felt justified to extrapolate the moment-curvature diagrams to failure on the basis of the shape of the corresponding load-midspan deflection curve. The extrapolated portions of the moment-curvature diagrams are shown by short-dashed lines in FIGURES 6.1 through 6.4 and in

FIGURES 7.1 through 7.4.

It should be noted that the curvatures which have been computed are "average" curvatures over a finite length of the beam and that the actual curvatures at a cracked section are significantly higher because of strain concentrations due to cracking. This is true even for the one-point loaded beams because even though the curvatures were computed for only the midspan section, the strains or deflections used to determine these curvatures were obtained over a finite length of the beam.

CHAPTER VII

DISCUSSION OF MOMENT-CURVATURE RELATIONSHIPS

7.1. Discussion of Measured Moment-Curvature Relationships

The moment-curvature relationships were very similar in shape to the load-midspan deflection curves. This is as expected because both the moment-curvature and the load-deflection relationships are dependent on the material properties of the beam. That is, both relationships are similarly affected by the cracking of the concrete, changes from elastic to inelastic behavior in both the compressed concrete and reinforcement, amount of reinforcement, level of prestress, concrete strength, and span length for the one-point loaded beams. The extent of the various stages of behavior for the load-deflection curve will vary according to the type of loading, but the moment-curvature relationship is not appreciably affected because it depends mainly on the magnitude of the applied moment.

As noted above the moment-curvature diagrams exhibited the three stages of behavior discussed in CHAPTER V which would seem to indicate that the moment-curvature relationship could be approximated, quite closely with three straight lines. This possibility was suggested in 1957, (2). The first straight line would represent the behavior from initial loading to first cracking. In this range the behavior of both the concrete and the reinforcement is elastic. The second straight line

would extend to initial yielding of the reinforcement. This range is marked by a transition in the behavior of the compressed concrete from elastic to inelastic with the reinforcement remaining elastic. The third straight line would extend to failure. This final range is characterized by inelastic behavior in both the concrete in compression and the reinforcement in tension. In this thesis no attempt was made to develop a procedure for determining such an idealized moment-curvature relationships.

7.2. Derivation of Theoretical Moment-Curvature Relationships

Theoretical "average" moment-curvature relationships were computed for all beams using the procedure outlined in (1), page 83 and 84. This method takes into account the effect of cracking, amount of reinforcement, concrete strength, the stress-strain characteristics for both the concrete and the reinforcement, and the level of prestress. The stress-strain relationship for the concrete was assumed to be composed of two straight lines. The equations of these lines are dependent on the concrete cylinder strength, f'_c, and are given in (1), page 79. The moment-curvature relationships obtained from this method are shown made up of a series of straight lines in FIGURE 7.1 through 7.4. The use of a curved line for the region above cracking was not justified because only a small number of points was determined for each beam.

7.3. Comparison of Theoretical and Measured Moment-Curvature Relationships

Comparisons between the moment-curvature relationships obtained from the measurement of deflections and from the procedure given in (1)

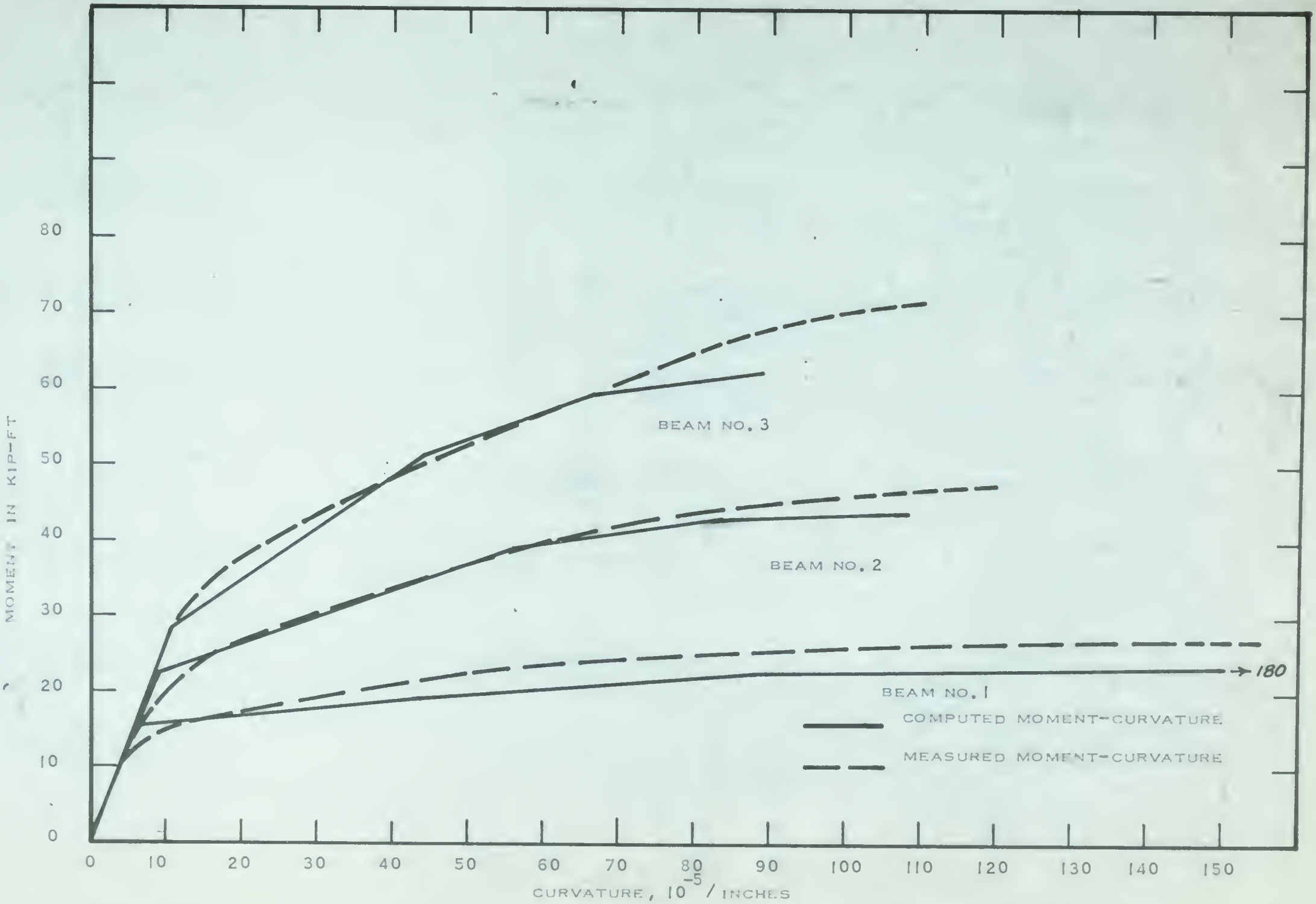

FIGURE 7.1. COMPARISON OF COMPUTED AND MEASURED MOMENT-CURVATURES

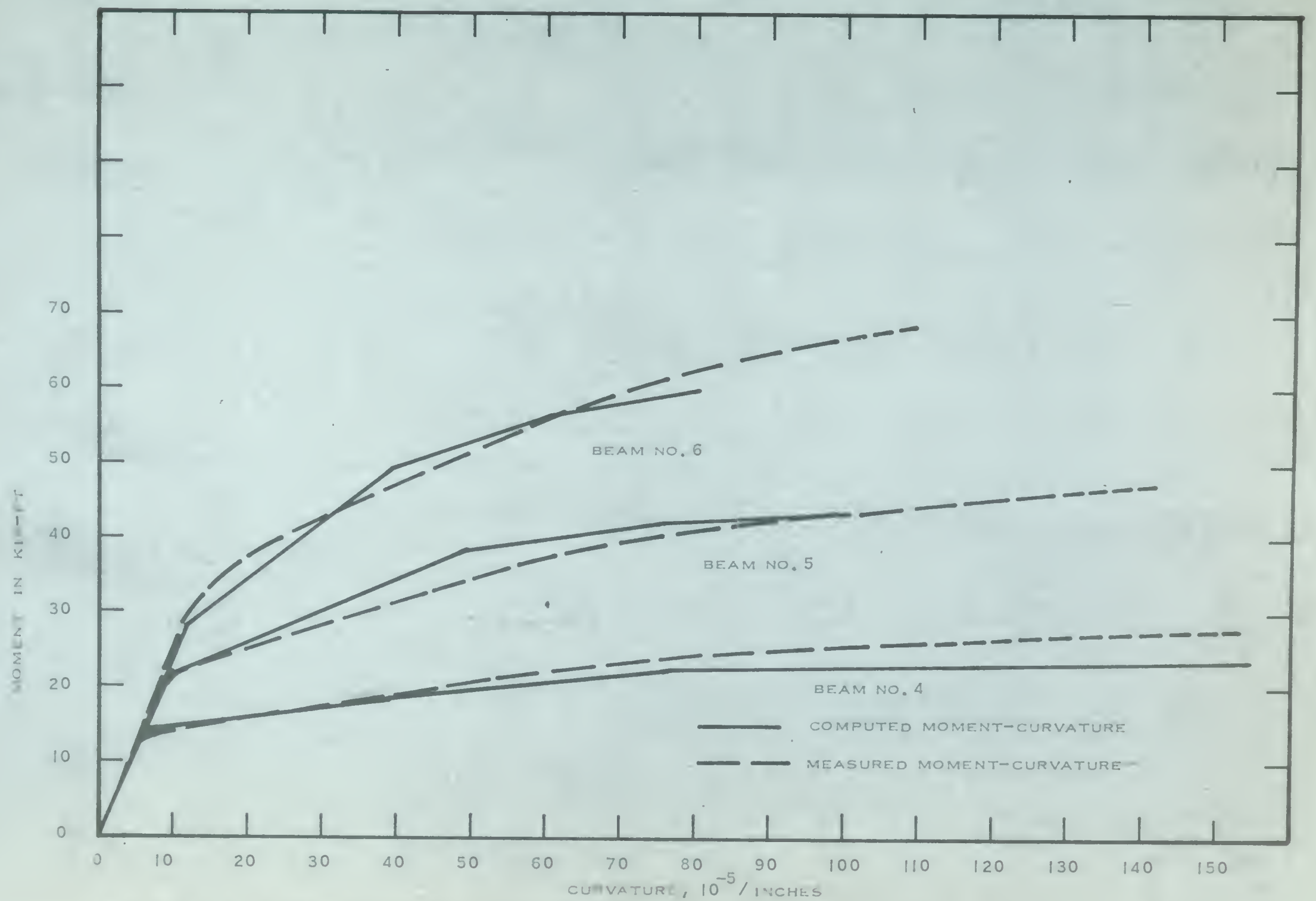

FIGURE 7.2. COMPARISON OF COMPUTED AND MEASURED MOMENT-CURVATURES

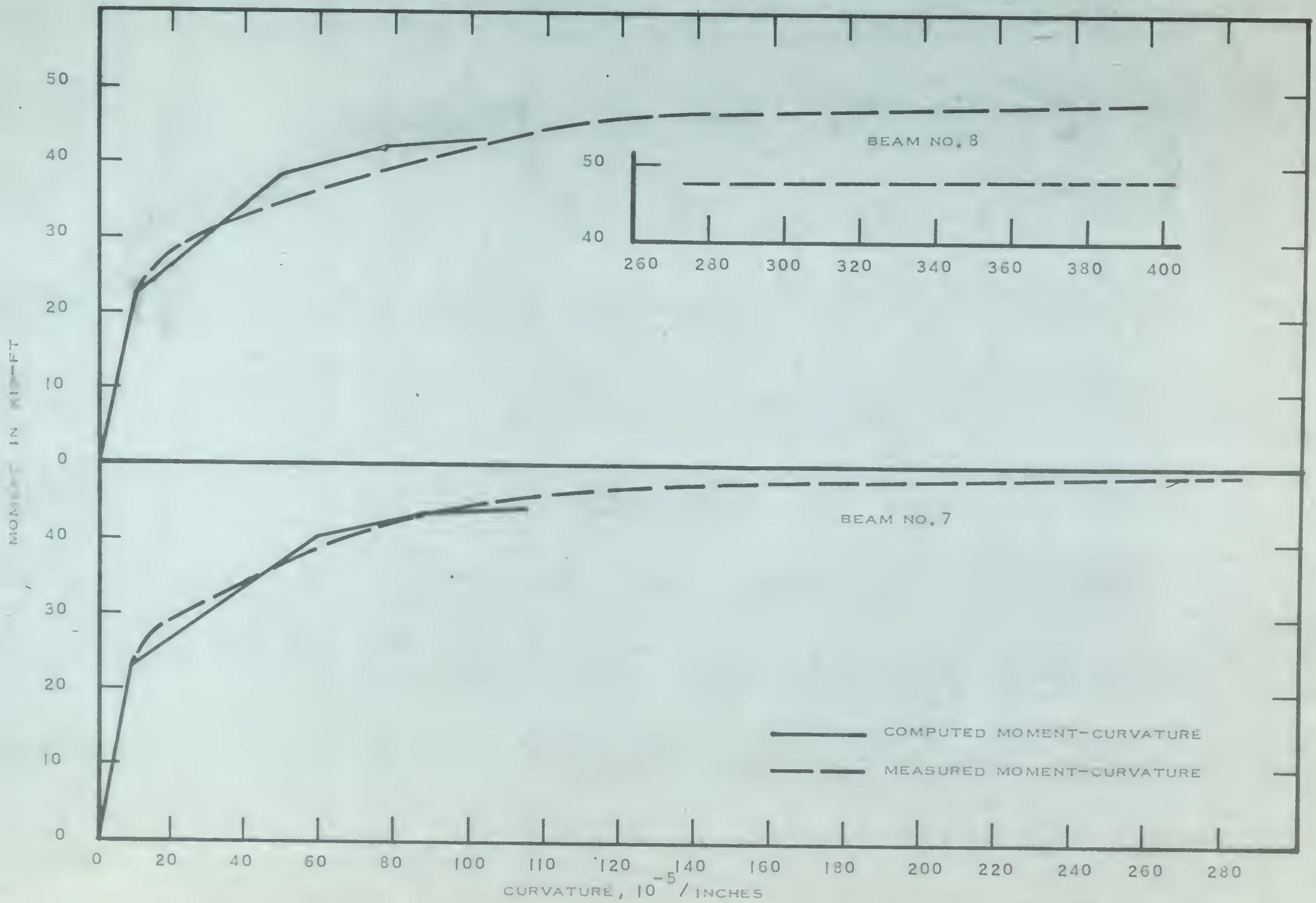

FIGURE 7.3. COMPARISON OF COMPUTED AND MEASURED MOMENT-CURVATURES

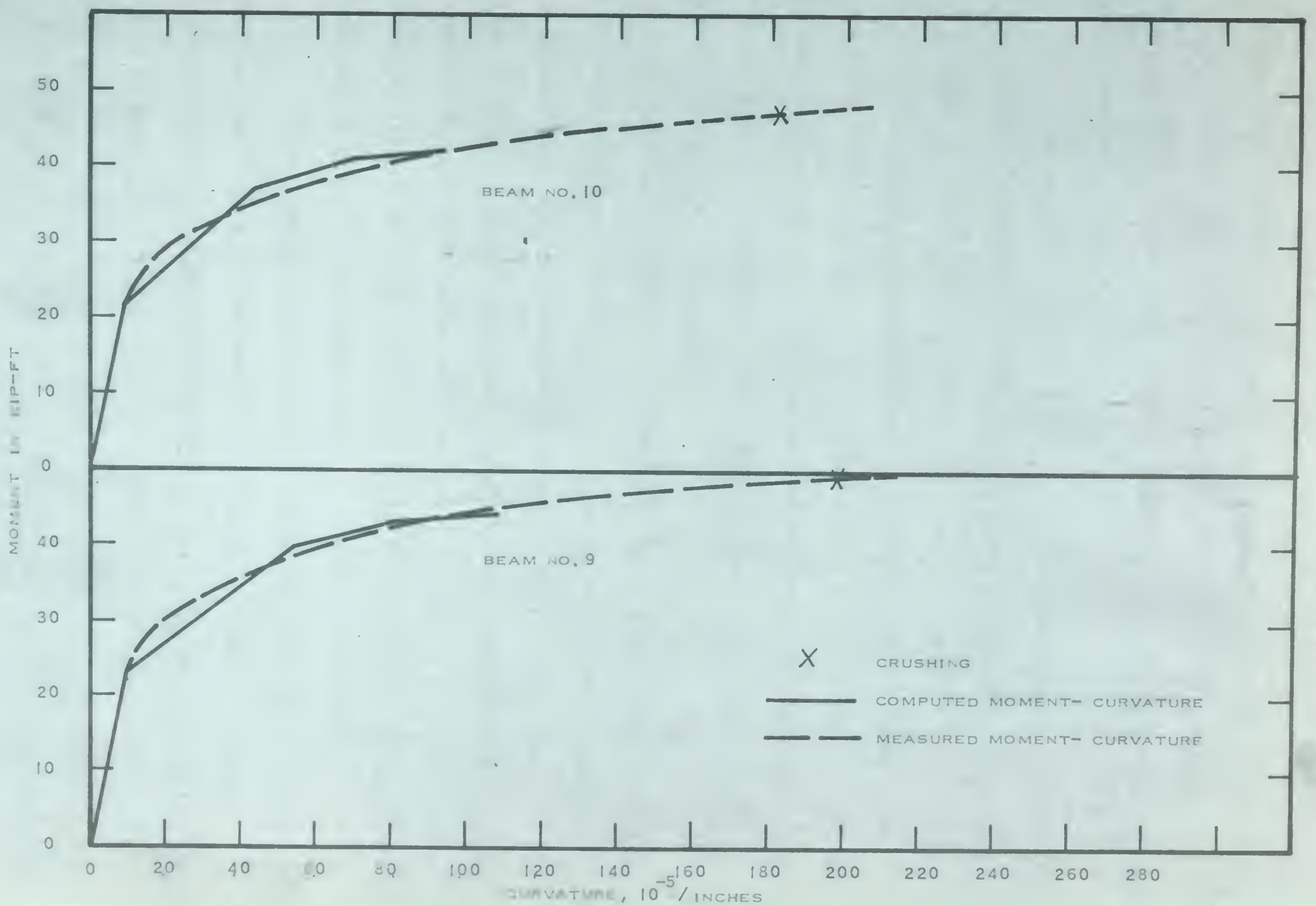

FIGURE 7.4. COMPARISON OF COMPUTED AND MEASURED MOMENT-CURVATURES

are shown in FIGURES 7.1 through 7.4. Considering all the beams, the correlation between the methods was quite good with the greatest discrepancies occurring for beams No. 1 and 4. Extremely good correlation was obtained for beam No. 2.

Any deviation of the theoretical moment-curvature relationship from the measured curve could be in either the computation of strength or curvature, or both. When comparing a pair of curves, it is impossible to differentiate between differences in strength and differences in curvature. This argument becomes meaningless, however, when the moment-curvature relationship becomes quite flat as for an under-reinforced in the third stage of behavior. Here, differences in curvature become irrelevant, except at failure.

The most significant differences between the theoretical and measured curves occurred over the second stage of behavior; generally, the theoretical curves were more steeply sloped over this range. This could be due, in part at least, to the choice of the simplified stress-strain relationship for the concrete which resulted in a greater apparent concrete strength over the transition range from elastic to inelastic behavior and also, in the latter portion of the inelastic range.

For all beams the measured ultimate strengths were 5 to 10 per cent higher than the theoretical. Such differences in strength occurred only in the latter portion of the moment-curvature diagrams except in beams No. 1 and 4 in which a difference of approximately 10 per cent existed almost from first cracking. These differences also could be attributed to the use of the simplified stress-strain relationship for concrete.

are shown in FIGURES 7.1 through 7.4. Considering all the beams, the correlation between the methods was quite good with the greatest discrepancies occurring for beams No. 1 and 4. Extremely good correlation was obtained for beam No. 2.

Any deviation of the theoretical moment-curvature relationship from the measured curve could be in either the computation of strength or curvature, or both. When comparing a pair of curves, it is impossible to differentiate between differences in strength and differences in curvature. This argument becomes meaningless, however, when the moment-curvature relationship becomes quite flat as for an under-reinforced beam in the third stage of behavior. Here, differences in curvature become irrelevant, except at failure.

The most significant differences between the theoretical and measured curves occurred over the second stage of behavior; generally, the theoretical curves were more steeply sloped over this range. This could be due, in part at least, to the choice of the simplified stress-strain relationship for the concrete which resulted in a greater apparent concrete strength over the transition range from elastic to inelastic behavior and also, in the latter portion of the inelastic range.

For all beams the measured ultimate strengths were 5 to 10 per cent higher than the theoretical. Such differences in strength occurred only in the latter portion of the moment-curvature diagrams except in beams No. 1 and 4 in which a difference of approximately 10 per cent existed almost from first cracking. These differences also could be attributed to the use of the simplified stress-strain relationship for concrete.

The additional strength, over the theoretical, which the beams exhibited was of a reasonable magnitude and even desirable from the standpoint of design. When a certain relationship, which has been derived on a theoretical-experimental basis, is applied to practice, the parameters of the relationship should account for the difference between conditions in the laboratory and those which exist ideally in the field. Though it is difficult to say exactly what ideal field conditions are, some of the factors which must be considered are: the fact that ideal loading conditions were used in the tests, there was good control of mix designs, actual concrete strengths were used in the derivation of the relationship, and the specimens were fabricated within relatively small tolerances.

A summary of the curvatures at or near ultimate for the two-point loaded beams is given in TABLE 7-1.

TABLE 7-1. CURVATURES AT OR NEAR ULTIMATE

Beam No.	Measured Curvatures		Theoretical Curvatures
	Last Recorded	Extrapolated to Failure	at Failure
	10^{-5}/in.	10^{-5}/in.	10^{-5}/in.
1	140	155	180
2	100	120	110
3	75	110	90
4	110	150	155
5	125	140	100
6	95	105	80

The theoretical curvatures compared favorably with the measured curvatures extrapolated to failure. For the beams having larger reinforcement ratios, the theoretical curvatures were significantly smaller than those measured at failure. This difference would probably be smaller if a more realistic stress-strain for concrete were used.

For the one-point loaded beams, the correlation between the theoretical and measured moment-curvature relationships over the major portion of loading was very good. This correlation does not mean, however, that the true moment-curvature relationship for the beams was obtained since neither method is justified in itself without the other. On the other hand, such correlation does increase the probability considerably that the curves were representative of the actual moment-curvature behavior in the beams. The measured curvatures at ultimate were much greater than the theoretical. This indicates that a beam has a much larger capacity to rotate if the failure is concentrated at one section than if failure can occur over a wide portion of the beam as for the two-point loaded beams. When failure is concentrated, stresses in the failure zone may be transferred to adjacent sections which are less strained. This is not possible in the two-point loaded beams because the entire middle span is subjected to the same moment. The rotation capacity of the one-point loaded beams was increased because of the confining effect of the bearing plate at midspan. In addition, the stirrups may have been closely enough spaced so that the confining effect was large enough to increase the rotation capacity. These factors were previously discussed in CHAPTER V regarding their effects on load-deflection curves.

CHAPTER V111

SUMMARY, CONCLUSIONS, AND RECOMMENDATIONS

8.1. Summary

Ten pretensioned prestressed concrete beams were tested under flexural loading. All beams had a 6 x 12-in. cross-section with an effective depth of 10 in. and were reinforced with 7-wire, 5/16-in. nominal diameter strand.

Six of the beams, having an 11-ft. span, were tested in pure flexure by loading at two points 3 ft. from each support. The variables for these beams were: percentage of reinforcement which ranged from 0.19 to 0.58 per cent, concrete strength, and an unintentional variation in the level of prestress which ranged from 120 to 142 ksi.

The remaining four beams were tested in moment combined with shear by loading at midspan only. For these beams the concrete strength was varied, as for the two-point loaded beams, and two span lengths of 11 ft. and 56 in. were used.

The measurements which were taken at each load increment are as follows: strains along the extreme fiber in compression, strains over the depth of the beams, and deflections along the bottom of the beams. The results of these measurements were used to compute curvatures which were combined with the corresponding moments. These moment-curvature relationships were compared with theoretical moment-curvatures determined from the procedure given in (1).

Pertinent characteristics of the behavior of the test beams are summarized as follows:

The following applies to the one-point loaded beams.

1. The load-midspan deflection curves for beams No. 9 and 10 exhibited a non-linear behavior over the second stage of behavior which was attributed to their short span length.

The following apply to the two-point loaded beams.

2. The deflections at ultimate of the higher reinforced beams were smaller, but of the same order as those of the lower reinforced beams.

3. Beams No. 1 and 4 reinforced with 2 strands failed by fracturing of the strand. These beams behaved in a ductile manner, exhibiting large deformations with little increase in load in the later stages of loading.

4. Beam No. 2 reinforced with 4 strands failed by a gentle crushing of the concrete. This type of failure indicated that the strengths of the compressed concrete and the reinforcement were nearly equal.

5. Beam No. 5 reinforced with 4 strands failed in quite an explosive manner when the concrete crushed. Beams No. 3 and 6 reinforced with 6 strands failed in a similar manner.

6. In the beams that failed by crushing of the concrete, no crushing was observed until just prior to failure.

7. The cracks were more closely spaced for beams with larger percentages of reinforcement. In addition, the cracks did not rise as high in these beams as in the beams with low percentages of reinforcement.

8. The distribution of strains along the top of the beams over the constant moment span were not uniform. This non-uniformity appeared to decrease as the amount of reinforcement in the beams increased.

9. The distribution of strains over the depth when averaged over four gage lines were found to be linear, even near failure.

8.2. Conclusions

On the basis of the results obtained from the beam tests, and a study of the behavior of the beams, the following conclusions have been drawn with regard to the behavior of bonded, prestressed concrete beams loaded in flexure:

1. A comparison of theload-midspan deflection curves and the measured moment-curvature relationships showed that the two types of load-deformation curves can be expected to be similar in shape regardless of the type of flexural loading over the normal range of beam length to depth ratios.

2. The load-deformation curves exhibited three distinct stages of behavior. The behavior over each stage was nearly linear.

The following conclusions apply to the two-point loaded beams.

3. The strength of the beams increased in almost a direct proportion to the amount of reinforcement.

4. The difference in failures between beams No. 2 and 5 was due to the strength of the concretes. The high concrete strength for beam No. 2 resulted in compressed concrete strength which was nearly equal to the strength of the reinforcement whereas the low concrete strength for beam No. 5 resulted in an over-reinforced beam.

5. Concrete strength had little effect on the behavior of the under-reinforced beams (Nos. 1 and 4) though the deflections over the second stage of behavior were slightly smaller for beam No. 1 which had the higher strength concrete.

6. The load required to produce initial cracking was higher for the beams having the larger amounts of reinforcement. This effect was a direct consequence mainly of the larger prestressing force.

7. The curvatures determined from the distribution of strains over the depth of the beams compared favorably with those determined from the deflections; though, the curvatures from the strains were generally somewhat smaller.

8. The theoretically derived moment-curvature relationships were found to correlate reasonably well with the moment-curvatures determined from the deflections. The theoretical curves were generally more steeply sloped over the second stage of behavior and underestimated the strength of the beams by 5 to 10 per cent.

The following conclusions apply to the one-point loaded beams.

9. The one- point loaded beams exhibited large deformations in the vicinity of midspan with little increase in load in the later stages of loading.

10. Cracking in the "long" beams (Nos. 7 and 8) extended over a wide portion of the beam while the "short" beams (Nos. 9 and 10) were marked by only three major cracks in the vicinity of midspan, with the outside cracks inclined toward the middle of the beam at approximately 60 degrees.

11. These beams all failed ultimately by fracturing of the strand. However, in each case failure of strand was preceded by crushing of the concrete. Considerable deformation took place after initial crushing of the concrete, expecially in the "short" beams.

12. The theoretically derived moment-curvature relationships compared well with those determined from the deflections over the major portion of loading. For the later stages of loading, the measured curvatures were much larger than those predicted.

8.3. Recommendations

With the completion of this study, the following regions appear to be open for further investigation in regard to deformation characteristics of prestressed concrete beams loaded in flexure:

1. Deformation characteristics of beams loaded at two points symmetrical about midspan using concrete strengths on the order of 3000 psi.

2. Effect of various types of reinforcement on the rotation capacity of sections subjected to pure flexure. Such reinforcement might include the use of deformed bars in the compression zone or closely spaced stirrups.

3. The effect on the behavior of one-point loaded beams of deformed bars in both the compression and tension zones over the central section of the beam.

4. Deformation characteristics of beams tested by loading at several locations along the entire span of the beam in order to approximate the effects due to a distributed load. The same magnitude of load could be applied to each location or the load could be varied from one location to the next.

LIST OF REFERENCES

1. Warwaruk, J., Sozen, M.A., Siess, C.P., "Strength and Behavior in Flexure of Prestressed Concrete Beams", University of Illinois Engineering Experiment Station Bulletin No. 464, August, 1962.

2. Macchi, Giorgio, "Moment Redistribution Beyond Elastic Limit and at Failure in Prestressed Concrete Beams", Journal of Prestressed Concrete Institute, Vol. 2, Sept., 1957, No.2.

3. Billet, D.F. and Appleton, J.H., "Flexural Strength of Prestressed Concrete Beams", Proceedings, American Concrete Institute, Vol. 50, 1954, p. 837.

4. Janney, J.R., Hognestad, E., and McHenry, D., "Ultimate Strength of Prestressed and Conventionally Reinforced Concrete Beams", Proceedings, American Concrete Institute, Vol. 52, 1955-56, p. 601.

5. Burns, Ned H., "Moment Curvature Relationships for Partially Prestressed Concrete Beams", Journal of the Prestressed Concrete Institute, February, 1964, Vol. 9, No. 1.

6. A.S.T.M. Designation: C 33-46.

7. Portland Cement Association, Canada Cement Company Limited, "Design and Control of Concrete Mixtures", 1950.

Appendix A

METHODS OF CALCULATION

A.1. Control Specimens

The compression strength of the concretes was determined from tests of 6 x 12-in. cylinders. Splitting-tests of 6 x 12-in. cylinders were used to determine tensile strength. The modulus of rupture was determined from 3 1/2 x 4 1/2 x 14-in. control beams loaded at the third points of a 12-in. span. The calculations involved are as follows:

(a) Compressive strength = Maximum load / cross-sectional area of cylinder

(b) Tensile strength = Maximum load / $\frac{\pi DL}{2}$

where: D = diameter of the cylinder

L = length of the cylinder

(c) Modulus of rupture = Maximum load x (2 in.) / $\frac{I}{y}$

where: I = moment of inertia of the cross-section about its centroidal axis

y = distance to the extreme fiber

A.2. Determination of Curvature from Measured Deflections for Beams with a Constant Moment Span

For the beams (Nos. 1 to 6 which had a span of constant moment, the deflected shape of the beam over this span was assumed to be that

of an arc of a circle. This is illustrated in FIGURE A.1. The circle passes through the origin and is tangent to the x - axis at $x = 0$.

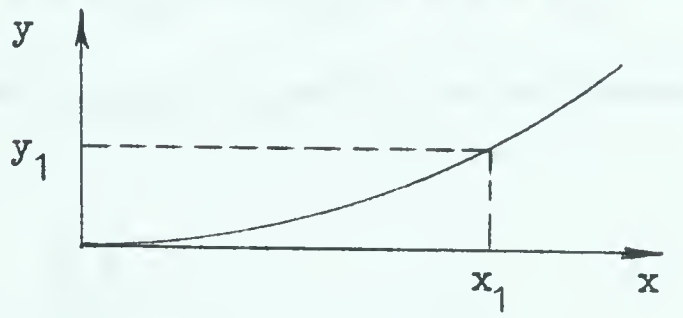

FIGURE A.1. ASSUMED DEFLECTED SHAPE OF BEAM

The equation for the circle is

$$x^2 + (y-R)^2 = R^2 \qquad (A.1)$$

where R = radius of the circle

When EQUATION A.1 is solved for R, the following is obtained

$$\frac{x^2+y^2}{2y} = R \qquad (A.2)$$

Thus, R can be calculated by substituting the values of the known coordinates (x_1, y_1) into EQUATION A.2. The curvature is equal to 1/R.

A.3. Determination of Curvature from Measured Deflections for Beams No. 7 and 8

For beams loaded at one point only, the bending moment diagram is made up straight lines which means that the rate of change of moment along the span is constant. By referring to EQUATION 3.10, it is shown that the rate of change of curvature must also be constant along the

span. Thus,

$$\frac{d}{dx}(1/R) = \frac{d^3y}{dx^3} = \text{constant} \qquad (A.3)$$

Integration of EQUATION A.3 three times with respect to x results in the following equation

$$y = C_1\frac{x^3}{6} + C_2\frac{x^2}{2} + C_3x + C_4 \qquad (A.4)$$

where C_1, C_2, C_3 and C_4 are constants of integration

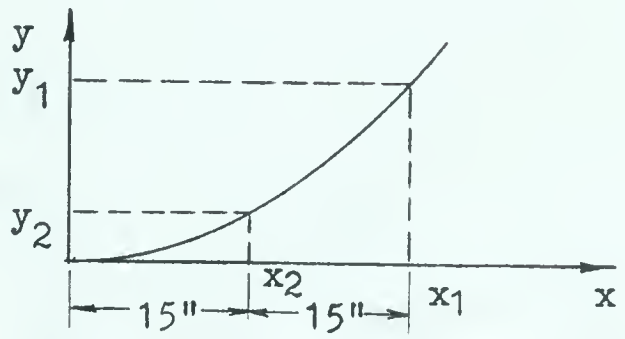

FIGURE A.2. ASSUMED DEFLECTED SHAPE OF BEAM

By referring to FIGURE A.2, the following boundary conditions are seen to apply:

(i) when $x = o$, $y = o$

(ii) when $x = o$, $\frac{dy}{dx} = o$

(iii) when $x = 1$ in., $y = y_2$

(iv) when $x = 30$ in., $y = y_1$

Substituting these boundary conditions into EQUATION A.4, the following values are obtained for the constants of integration:

$$C_1 = \frac{y_1 - 4y_2}{2250} \qquad C_2 = \frac{8y_2 - y_1}{450} \qquad C_3 = C_4 = 0$$

The equation for curvature is then obtained by substituting these constants into EQUATION A.4 and differentiating twice with respect to x. The curvature at midspan is obtained by setting $x = o$.

A.4. Determination of Curvature from Measured Deflections for Beams No. 9 and 10

The equation for the parabola shown in FIGURE A.3 is

$$y = Ax^2 \tag{A.5}$$

where A is a constant

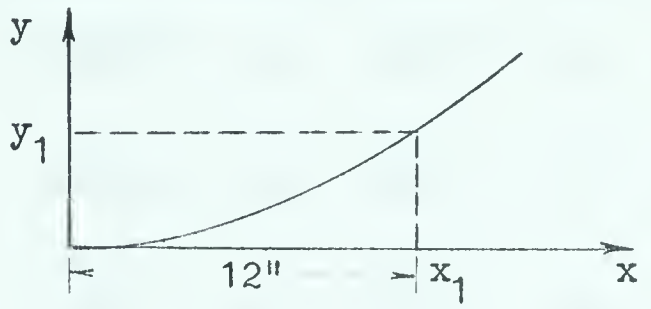

FIGURE A.3. ASSUMED DEFLECTED SHAPE OF BEAM

The constant, A, is determined from the known coordinates (x_1, y_1). The curvature at midspan is then determined by differentiating EQUATION A.5 twice with respect to x.

A.5. Determination of Prestress Loss

In computing the theoretical moment-curvature relationships, it was necessary to know the effective prestress at the time the beam was tested. From the time of initial prestressing to the time of casting, losses were measured with the dynamometers. From the time just prior to release of the prestress to the time of test, an indication of the losses was determined by measuring the concrete strains at the level of the reinforcement. The strains were measured with a Demec gage. Measurements were taken just before release, just after release, and at the

time of test. A summary of the measured losses of prestress are given in TABLE A-1. The initial prestress, as shown in TABLE A-1, is the value of prestress just prior to casting of the beam.

TABLE A-1. LOSS OF PRESTRESS IN THE REINFORCEMENT

Beam No.	No. of Strands	Average Initial Prestress	Average Elastic Shortening		Average Creep & Shrinkage		Total Loss		Effective Prestress
		(Ksi.)	(in/in.)	(Ksi)	(in/in.)	(Ksi)	(in/in.)	(Ksi)	(Ksi)
1	2	160.8	.00020	5.4	.00050	13.5	.00070	18.9	142
2	4	161.5	.00041	11.1	.00063	17.0	.00104	28.1	133
3	6	156.0	.00057	15.5	.00077	20.8	.00134	36.3	120
4	2	158.6	.00024	6.5	.00050	13.5	.00074	20.0	139
5	4	157.2	.00048	13.0	.00056	15.0	.00104	28.0	129
6	6	159.1	.00070	18.9	.00064	17.3	.00134	36.2	123
7	4	157.7	.00036	9.7	.00055	14.8	.00091	24.5	133
8	4	156.8	.00038	10.2	.00051	13.8	.00089	24.0	133
9	4	158.4	.00037	10.0	.00054	14.6	.00091	24.6	134
10	4	158.4	.00043	11.6	.00053	14.3	.00096	25.9	133

Note: in converting strain to stress, a value of $E = 27 \times 10^6$ psi was used.

Appendix B

PRESTRESSING EQUIPMENT

B.1. Dynamometers

The dynamometers consisted of small aluminum cylinders which fit loosely over the strand. They were mounted between the grip and the bearing plate located at the end opposite to that at which the tension was applied. The tension force in the strand was determined by measuring the compressive strain in the dynamometer. Strain was measured by means of two SR-4 electrical strain gages mounted at mid-length and diametrically opposite to each other and wired in series. This arrangement gave a strain reading which was the average of the strains measured by the two gages, thereby balancing the effects due to any small eccentricities of load that might occur. A typical dynamometer is detailed in FIGURE B.1.

The problem in the design of the dynamometers was to obtain the greatest sensitivity to changes in force. This required that the strains should be as large as possible for a given applied force. In regard to the type of material which should be used, this condition would be met if the material had both a low modulus of elasticity and adequate strength. In regard to size, the net cross-sectional area should be a minimum and yet maintain an adequate factor of safety during the prestressing operation, with respect to the yield point of the material. In addition, as implied above, the material should obey Hooke's Law in the region of operation. A high strength aluminum met these requirements very well; however, the

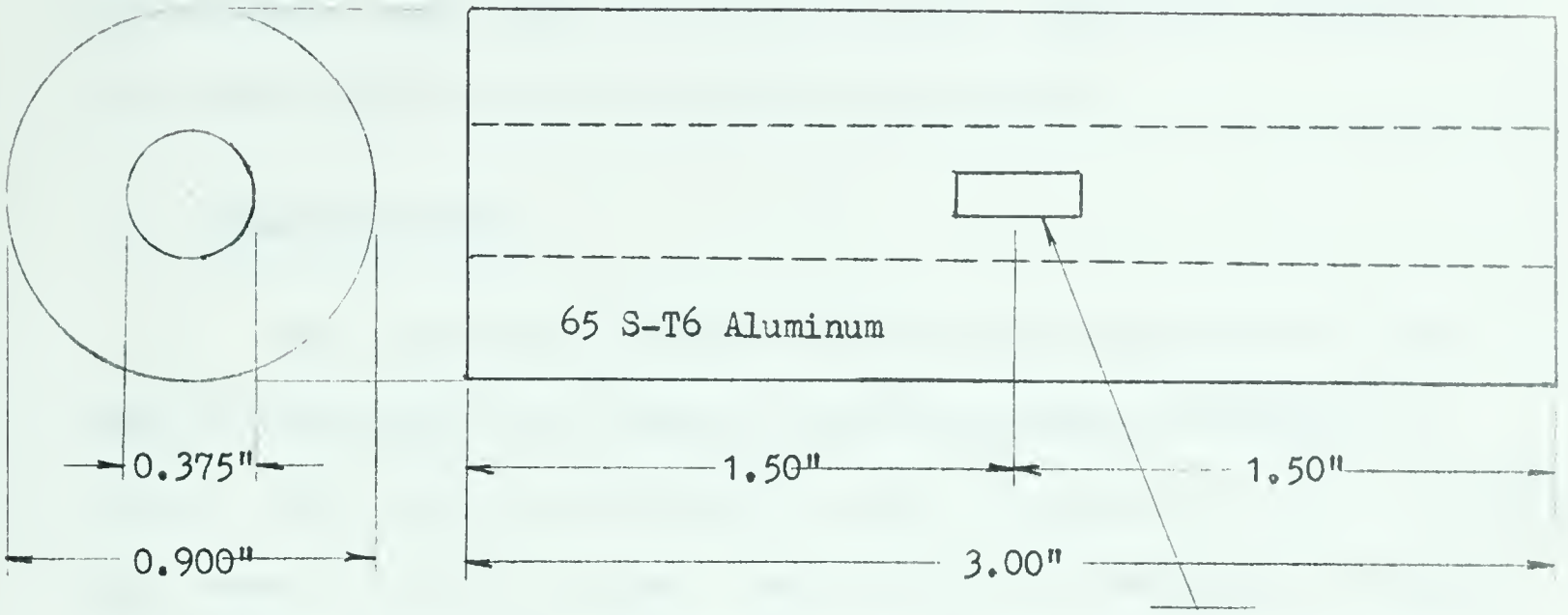

Net area = 0.5257 $in.^2$

For force of 15 kips, stress = 28.6 ksi

Assuming E = $10x10^6$ psi, $1x10^{-6}$ in. of strain corresponds to 5.26 lb. of force.

SR-4 Strain gage
Type A-5
Resistance = 120.4 ± .2
120.0 ± .2
Gage factor = 2.02 ± 1 %
Lot No. B31

FIGURE B.1. DETAILS OF A DYNAMOMETER

governing factor was the availability of material and consequently, 65 S-T6 aluminum with a 0.2 per cent yield strength of approximately 40 ksi was used.

The dynamometers were calibrated in a hydraulic testing machine. Before the actual calibration, the dynamometers were loaded through three cycles from zero to the highest load and back to zero. This was done to try to minimize hysteresis effects due to the cyclic loading which the dynamometers would be subjected to during their use. Calibration was performed by continuous loading with the strains being recorded at certain intervals until the maximum required load was reached. A greater number of dynamometers than was actually required

was calibrated since some were found to give a significant scatter of points when plotting the load-strain relationship.

B.2. Prestressing Bed

Two reinforced concrete end blocks were constructed at the start of the project, the details of which are given in FIGURES B.2 and B.3. Each block was designed to resist a horizontal force of 140 kips and a moment of 2300 in. kips. Four-1 1/12-in. diameter high strength bolts, pretensioned to approximately 60 ksi, were used to anchor each block to the loading bed. The blocks were set in mortar to provide uniform bearing between the bottom of the block and the floor. The anchor bolts were pretensioned so that, when prestressing, the prestress force would be transferred from the block through friction to the floor as opposed to direct bearing and shear on the anchor bolts. The jacking arrangement for pretensioning the anchor bolts is shown in FIGURE B.4. An overall view of the prestressing bed is shown in FIGURE B.5.

Both blocks were designed with a central longitudinal channel 1-ft. in width and almost the full height of the block to allow the strands to pass through. This channel was spanned at the two ends of the bed by a horizontal layer of plates, 7" x 3/4" x 2' - 6", spaced apart by 7" x 3/8" x 0'-9" plates located on both sides of the channel and by a 3/8-in. vertical bearing plate across the faces of the former set of plates. This arrangement of plates is shown in FIGURES 4.3 and 4.4. Provision had been made for the use of any number of the spanning plates, i.e. any number of layers of strand, and the whole assembly could be positioned at any height on the end block.

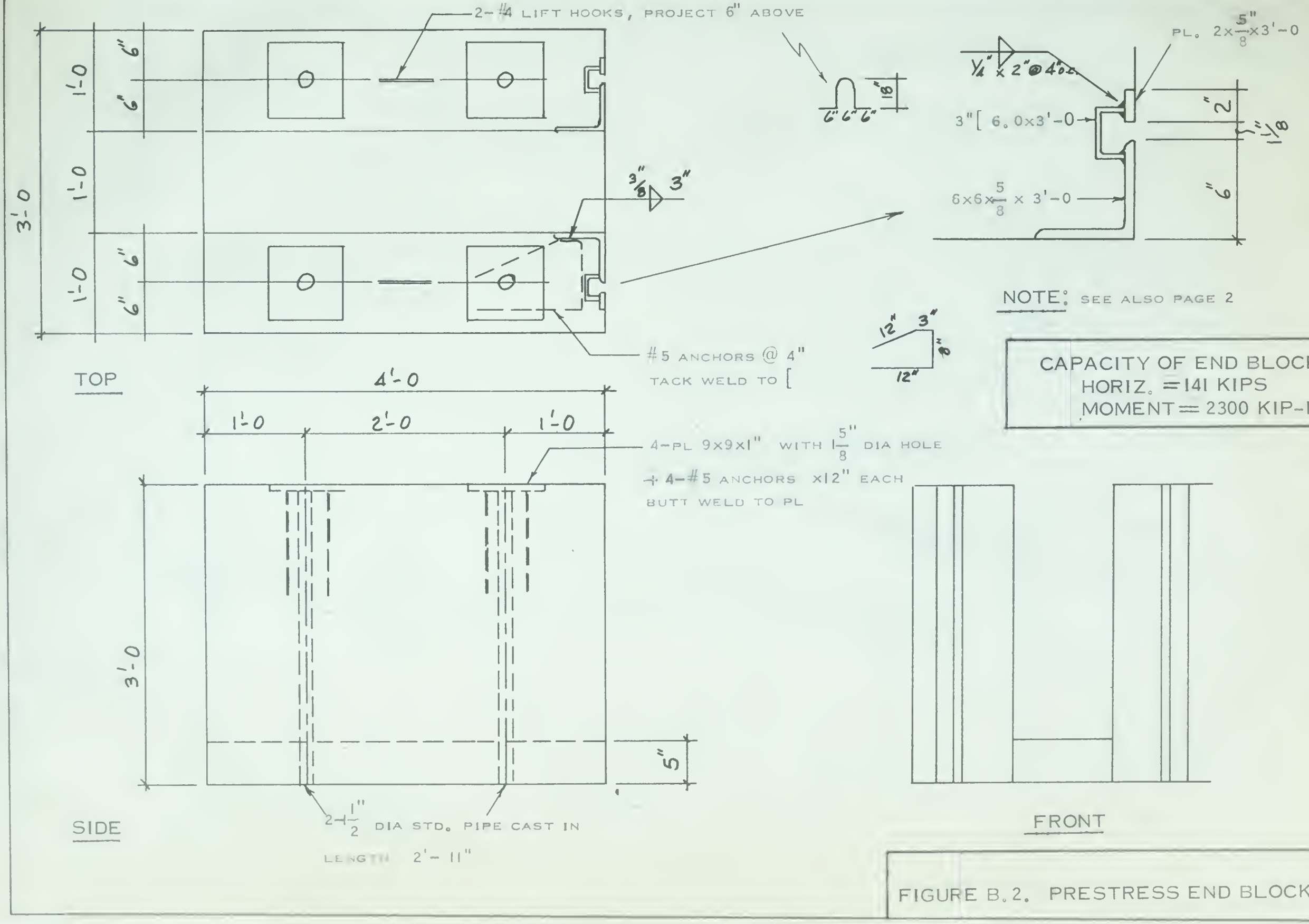

CAPACITY OF END BLOCK
HORIZ. = 141 KIPS
MOMENT = 2300 KIP-IN

FIGURE B.2. PRESTRESS END BLOCKS

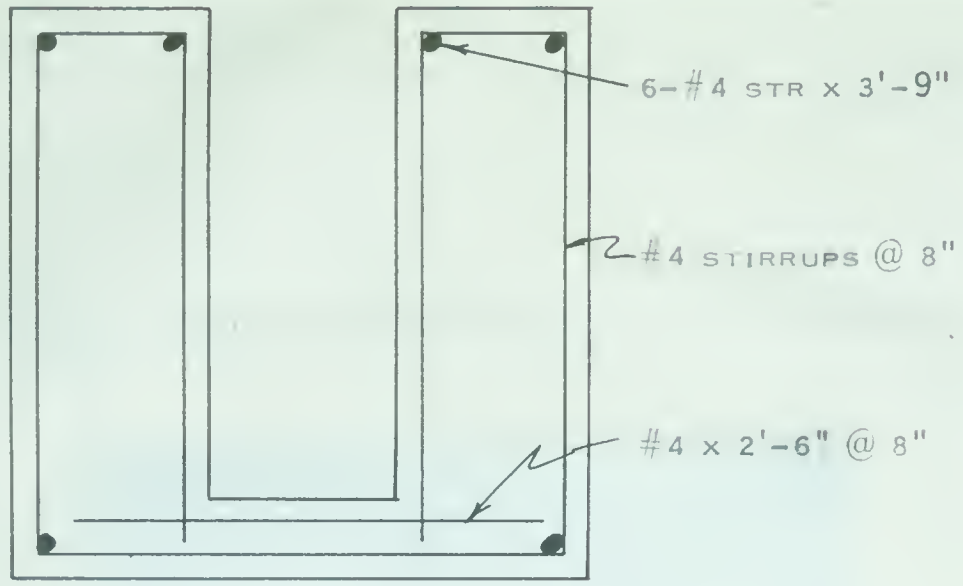

REINFORCING SECTION

COVER $1\frac{1}{2}$" MIN

RE-BAR SCHEDULE

TOTALS FOR 2 BLOCKS

12-#4 STR x 3'-9"
14-#4 STR x 2'-6"
14-#4 STIRRUP x 14'-10$\frac{1}{2}$"
32-#5 STR ANCHORS x 12"
40-#5 BENT ANCHORS x 2'-11"
4-#4 ANCHORS 4'-6"

MISC. IRON SCHEDULE

TOTALS FOR 2 BLOCKS

8 PL 9x9x1"
4 6x6x$\frac{5}{8}$ x3'-0
4 PL 2x$\frac{5}{8}$ x 3'-0
4-3" [6.0 x 3'-0
8-1$\frac{1}{2}$ IN. STD PIPE X 2'-11"

PRESTRESS END PLS AND SPACER PLS TO BE USED ON PROJECT BY GEORGE RAFFA

24 SPACER PLS 7x$\frac{3}{8}$ x9"
12-PL 7"x$\frac{3}{4}$" x 2'-6" NOTE HIGH STRENGTH STEEL
12- 1" DIA STD BOLTS X 12" C/W NUT AND WASHER 6" THREAD

MAKE 2 END BLOCKS

FOR ATTACHING TO FLOOR, USE 1$\frac{1}{2}$ IN. H.T. BOLTS X 6'-6", EACH PRESTRESSED TO 71,000 LB.

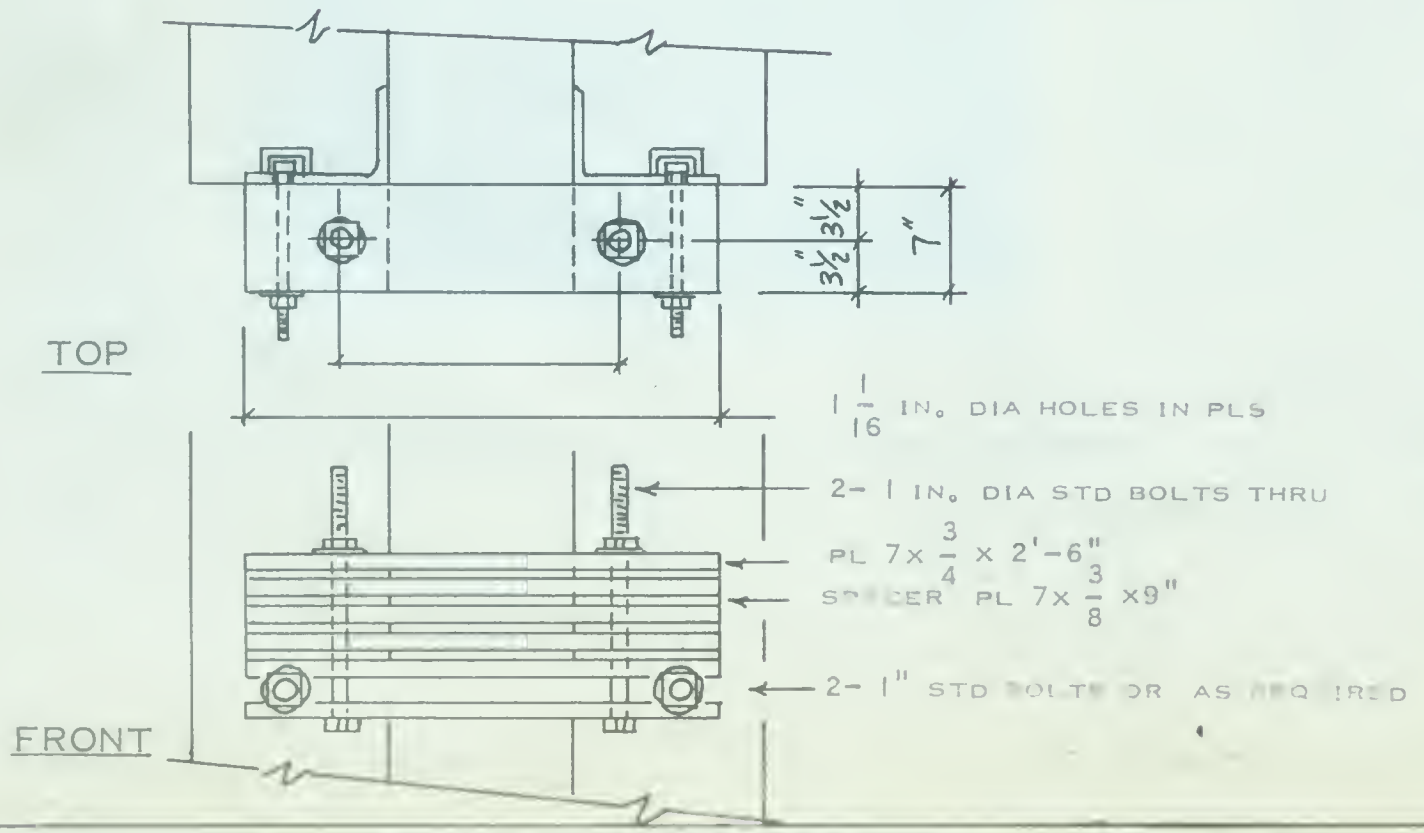

FIGURE B.3. PRESTRESS END BLOCKS

FIGURE B.4. JACKING ARRANGEMENT FOR PRESTRESSING ANCHOR BOLTS

FIGURE B.5. OVERALL VIEW OF PRESTRESSING BED WITH LOADING APPARATUS IN THE BACKGROUND